

Carbon-based adsorbents for fluoroquinolone removal in water and wastewater: A critical review

Published in: *Environmental Research*

Citation for published version: Ashiq, A., Vithanage, M., Sarkar, B., Kumar, M., Bhatnagar, A., Khan, E., Xi, Y., Ok, Y.S. (2021) Carbon-based adsorbents for fluoroquinolone removal in water and wastewater: A critical review. *Environmental Research*. 197: 111091. doi: 10.1016/j.envres.2021.111091.

Document version: Accepted peer-reviewed version.

**Carbon-based adsorbents for fluoroquinolone removal in water and wastewater: A
critical review**

Ahmed Ashiq¹, Meththika Vithanage^{1*}, Binoy Sarkar², Manish Kumar³, Amit Bhatnagar⁴,
Eakalak Khan⁵, Yunfei Xi⁶, Yong Sik Ok^{7**}

¹Ecosphere Resilience Research Centre, Faculty of Applied Science, University of Sri
Jayewardenepura, Sri Lanka

²Lancaster Environment Centre, Lancaster University, Lancaster, LA1 4YQ, United
Kingdom

³Department of Earth Sciences, Indian Institute of Technology Gandhinagar, India

⁴Department of Separation Science, LUT School of Engineering Science, LUT University,
Sammonkatu 12, FI-50130, Mikkeli, Finland

⁵Civil and Environmental Engineering and Construction Department, University of Nevada –
Las Vegas, Las Vegas, NV, USA

⁶Institute for Future Environments & School of Earth and Atmospheric Sciences, Queensland
University of Technology (QUT), 2 George Street, Brisbane, Queensland 4001, Australia

⁷Korea Biochar Research Center, APRU Sustainable Waste Management Program &
Division of Environmental Science and Ecological Engineering, Korea University, Seoul,
Korea

*Corresponding Author: meththika@sjp.ac.lk

**Co-Corresponding Author: yongsikok@korea.ac.kr

38	Abstract	4
39	1. Introduction	5
40	2. Fluoroquinolone antibiotics: properties and persistence in the environment ...	8
41	2.1. Properties of fluoroquinolone antibiotics	8
42	2.2. Occurrence and distribution of FQ antibiotics in the environmental matrices	9
43	2.2.1. <i>Soil-plant system</i>	9
44	2.2.2. <i>Water and wastewater</i>	10
45	2.2.3. <i>Persistence of FQs in the environment</i>	15
46	3. Adsorption of FQs by carbon-based, tailored and other material adsorbent .	19
47	3.1. Carbon-based adsorbents for FQs removal	20
48	3.1.1. <i>Activated carbon</i>	20
49	3.1.2. <i>Biochar</i>	26
50	3.1.3. <i>Graphene-based adsorbents</i>	31
51	3.1.4. <i>Carbon nanotubes</i>	34
52	3.2. Adsorptive removal of FQ antibiotic by clay and tailored adsorbents	38
53	3.2.1. <i>Clay adsorbents</i>	38
54	3.2.2. <i>Carbon composites</i>	41
55	3.2.3. <i>Other nano-based composites</i>	43
56	5. Performance evaluation of FQ removal	51
57	References	58
58		

60 This review summarizes the adsorptive removal of Fluoroquinolones (FQ) from water and
61 wastewater. The influence of different physicochemical parameters on the adsorptive removal
62 of FQ-based compounds is detailed. Further, the mechanisms involved in the adsorption of FQ-
63 based antibiotics on various adsorbents are succinctly described. As the first of its kind, this
64 paper emphasizes the performance of each adsorbent for FQ-type antibiotic removal based on
65 partition coefficients of the adsorbents that is a more sensitive parameter than adsorption
66 capacity for comparing the performances of adsorbents under various adsorbate concentrations
67 and heterogeneous environmental conditions. It was found that π - π electron donor-acceptor
68 interactions, electrostatic interactions, and pore-filling were the most prominent mechanisms
69 for FQ adsorption by carbon and clay-based adsorbents. Among all the categories of adsorbents
70 reviewed, graphene showed the highest performance for the removal of FQ antibiotics from
71 water and wastewater. Based on the current state of knowledge, this review fills the gap through
72 methodologically understanding the mechanism for further improvement of FQ antibiotics
73 adsorption performance from water and wastewater.

74 **Keywords:** Emerging contaminants, clean water and sanitation, green and sustainable
75 remediation, carbon-based adsorbents, sustainable development goals, nanomaterials.

1. Introduction

The availability of clean drinking water is becoming steadily more challenging in many parts of the world, especially in countries in Asian and African countries. Seventy percent of the global economic inputs lies in cities and urban areas where a large number of the population is vulnerable in accessing clean water and sanitation. United Nations' Sustainable Development Goals (SDG 6 for clean water and sanitation) advocate ensuring access to clean water supply, appropriate sewage and sanitation facilities to all [1]. However, from the past few decades, pharmaceuticals and personal care products (PPCPs) have become an emerging concern because of their pseudo-persistent nature and continuous input to the environment [2,3]. Large quantities of antibiotics are excreted, mainly whose active ingredient remains unaltered after absorption by the human body, leading to exposure to bacteria in the environment, which has resulted in antimicrobial resistance [4,5]. The antibiotics released into the water bodies are of great concern because they: (i) cause water and soil contamination in trace amounts posing risks to human and animal health through entry into the food-chain; (ii) enhance bacterial resistance in the aquatic bodies, and (iii) inhibit or kill certain beneficial bacteria in natural ecosystems [3,6].

Quinolone is a crucial class of antibiotic used to treat both veterinary and human diseases because of its ability to control both Gram (+) and Gram (-) bacterial infections. Derivations of quinolone include fluorination at the 6th -position of the parent compound resulting in fluoroquinolone (FQ) antibiotic, a predominant quinolone type [7,8]. Furthermore, 70% of the FQ consumed is excreted unmetabolized from the body, and is frequently detected at sub-inhibitory concentrations ranging from ng L⁻¹ to µg L⁻¹, which can thereby accumulate and facilitate long-term exposure. Thus, FQ could alter the natural microbial populations in soil and water [9].

The amount of published literature to remediate FQ from aqueous media has increased rapidly since 2011, as shown in Figure 1. Many conventional strategies have been employed to remove FQs from aqueous environments such as biological processes, sand filtration, ultraviolet (UV) radiation, membrane filtration and/or sedimentation (Figure 1) [10–12]. Among these techniques, biodegradation and adsorption have gained momentum in the last few years. The oxidation process generally utilizes UV or strong oxidants with severe operating conditions. Moreover, these methods have not been found to be practical for ionizable and polar contaminants such as FQ antibiotics. Despite numerous studies where conventional methods were carried out to remove FQ antibiotics, remediation of multiple FQ at varying pH values with specialized adsorbents and performance of each of them remains limited [13,14]. Research over the past decades has been dedicated to study the viability of numerous adsorbent materials including activated carbon, carbon nanotubes, clay minerals, ion exchange resins, and biochar for the removal of FQs. However, there is no review dedicated exclusively to FQ antibiotics. A dedicated review on adsorptive removal of FQ-antibiotics is necessary because identifying and categorizing the merits and demerits of various adsorbents are needed [15–19]. This sparked the necessity for using carbon-, nanocomposite-, and clay-based advanced adsorbents to remediate FQs in aqueous media. Thus, in this review, we intend to provide a complete overview of the studied adsorbents for remediating FQ-antibiotics with a comparative description based on the evidence retrieved from the overall performance of each of the adsorbents.

This review will help understand the adsorption phenomena at solid-solution interfaces using the adsorbents, as mentioned earlier, to abate aqueous FQ contaminations. Furthermore, it critically assesses the knowledge gaps and uncertainties concerning the merits and demerits of each type of adsorbent. In addition to adsorption capacity, we use partition coefficient as a performance assessment indicator to obtain a fair and critical comparison of FQ removal

performances using various adsorbents under different initial conditions. Based on the literature findings, we put forward some future research directions for further technological improvement of FQ removal from water and wastewater.

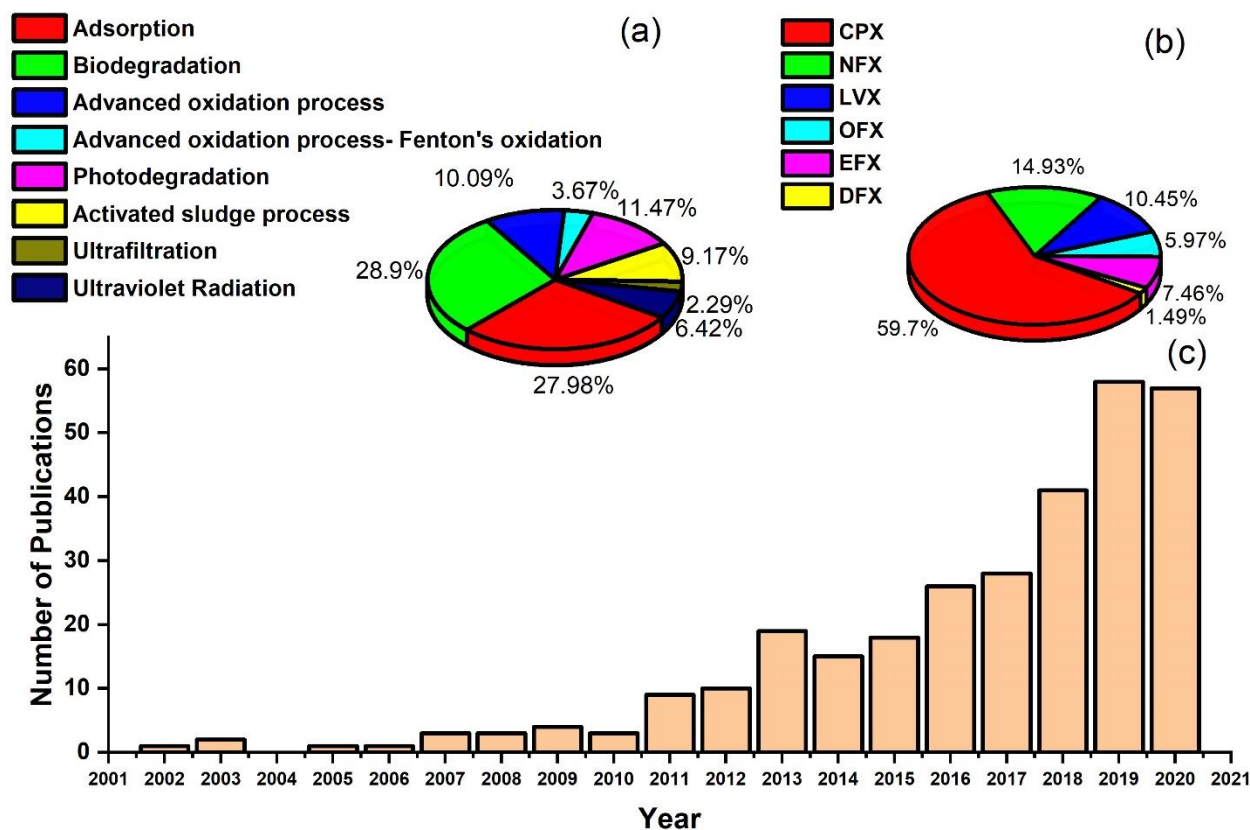


Figure 1: (a) Pie chart showing the corresponding % of each FQ remediation technique published during the past years (2001-2020), with “Fluroquinolone removal water” and “Quinolone removal water” as qualifiers. (b) Pie chart showing the corresponding % of each FQ studied here accumulated from tables presented in this study. (c) Number of publications on the adsorption of FQs from aqueous media per year since 2001 to 2020 extracted from Scopus with the key words “Fluroquinolone adsorption water” and words “Quinolone adsorption water”.

2. Fluoroquinolone antibiotics: properties and persistence in the environment

2.1. Properties of fluoroquinolone antibiotics

Approximately 25 years ago, the first mono-fluorinated FQ was developed from flumequine, which is a nalidixic acid with a limited antibacterial spectrum. Then, the addition of fluorine in the flumequine resulted in the development of novel FQs depending upon the clinical needs [20]. The novel FQ synthesized had nitrogen at N-1, carboxylic acid at C-3, ketone at C-4 and fluorine at C-6 of the compound's backbone structure. For some FQs, a unique piperazinyl group at C-7 provides them with unique antibacterial effects [21,22]. The minimum necessary structure for the activity in an FQ antibiotic is a 2-phenyl-4-pyridone-3-carboxylic acid, and the nitrogen can be displaced with other functional groups that must be below the plane of pyridine for optimal antibacterial effects [20].

Most FQs exhibit high chemical stability and are insensitive to degradation by hydrolysis and temperature. However, they can get substantially degraded by UV light. Their antibiotic competency depends on the available fluorine substituents at the 6th carbon position [23,24]. The addition of a fluorine group at C-6 and a piperazinyl group at C-7 makes FQs highly unique compared to other types of quinolone. Intrinsic anti-Gram (-) bacterial activity is shown by all quinolone-type antibiotics; however, FQ has the advantage of increased lipophilicity that gives them a higher tendency for anti-Gram (+) bacterial activity [22,25]. New FQs are being developed based on the chirality of the molecule for enhanced antibacterial activity. Ofloxacin, a tricyclic compound with methyl-group at the C-3 position, is an enantiomer of levofloxacin, which is 8-28 times more potent than ofloxacin. Such FQ was discovered based on the already available type and its mode of response by the receptors such as animals, poultry and fish. In most cases, the newly developed antibiotics are utilized for the treatment of pulmonary, urinary, and digestive infections [22,26]. Enrofloxacin and sarafloxacin are used in veterinary

medicines; ciprofloxacin, norfloxacin, and ofloxacin are used in human medicines. Ciprofloxacin is one of the most prominently used antibiotics worldwide [27,28].

2.2. Occurrence and distribution of FQ antibiotics in the environmental matrices

Elevated concentrations of FQ antibiotics are present in the environmental matrices and are closely associated with their release from hospital waste effluents, veterinary activities and untreated sludge from pharmaceutical industries [29–32]. Table 1 summarizes the prevalence of FQ antibiotics in soil, water, sludge and few food crops indicating their frequent occurrences and concentrations. From previous studies on the occurrence of FQ in soil, water, sludge and manure in different countries and regions, the antibiotics have been mapped based on the mean values of their occurrences in each country to show the global distribution of FQ (Figure 2).

2.2.1. Soil-plant system

Because of the pseudo-persistent nature of FQ antibiotics in the environment, their fate in the plant and soil systems is complex, and thus, creates a menace in the agroecosystems. Agricultural soils acquire antibiotics from wastewater and offsite runoff, which get bio-accumulated in the plant tissues over time [4,33]. Mechanisms for the translocation of FQ antibiotics in plants depend on multiple factors, mainly soil properties and the nature of antibiotics. The transport of nutrients, water, and other compounds from plant root to shoot occurs through the xylem [34,35]. After being absorbed by plants from soil, FQ antibiotics are converted to zwitterionic species at neutral pH and accumulate in leaves where the pH of vacuoles, xylem cells, and intercellular spaces is around 5 to 6. The ionizing effect of FQ antibiotics varies with changing environments in the contaminated water. Because of the gradient created in the solute, the accessibility of FQ antibiotics towards the rest of the plant system becomes effortless [23,36,37]. However, other antibiotics (e.g., tetracycline and penicillin) do not get transported in plant bodies due to having higher octanol-water partition

coefficient values than FQs (Table 2). Tetracycline and penicillin are detected in the root system only, while FQs are found in different parts of the plants [21,38,39]. Edible plant parts are thus prone to FQ bioaccumulation and aggravate human exposure through food consumption. Chinese white cabbage, spinach, radish and corn crops, irrigated with antibiotic-contaminated wastewater over an extended period, were reported to cause FQ exposure to humans through edible plant parts [37], increasing the ecotoxicity in soil and plant matrices.

2.2.2. *Water and wastewater*

Quinolones have been detected in surface waters up to $2 \mu\text{g L}^{-1}$ with a detection frequency of 15-83% globally. About 4 ng L^{-1} norfloxacin was detected in the agricultural run-off in Hong Kong [40]. Norfloxacin (NFX), lomefloxacin (LMX), enrofloxacin (EFX), and ciprofloxacin (CPX) were found in tap water samples up to 680 ng L^{-1} (77.5% frequency) and $2\text{-}40 \text{ ng L}^{-1}$ (100% frequency) in Guangzhou and Macao, respectively [40,41]. In New Mexico, ofloxacin ranging from $0.1\text{-}0.5 \mu\text{g L}^{-1}$ was detected in the effluent wastewater treatment plants with 100% frequency [40]. The transformed metabolites could worsen the ecotoxicity in the effluents of the untreated water treatment plants throughout the course of FQ presence in water [35,42]. Overall, FQs are becoming almost ubiquitous in nature due to their constant release in excreted metabolites from domestic households to the environment [42,43].

The metabolite of enrofloxacin used as an animal drug undergoes a change in the structure through N-dealkylation of the piperazine ring in the animal body to another commonly excreted fluoroquinolone, ciprofloxacin. N-acetyl ciprofloxacin is detected as a metabolite found in the environment along with enrofloxacin N-oxide and diethylene-enrofloxacin for the same parent compound, enrofloxacin [26,44]. Although their consequences in the ecological environment can be less toxic than their parent compounds, they can accumulate in trace amounts [45]. Both

209 metabolized or un-metabolized FQ antibiotics reach the soil through animal wastes and are
210 easily transported to ground and surface waters.

211 Ciprofloxacin, norfloxacin and ofloxacin are more predominant in aquatic environments than
212 the other FQs. Norfloxacin and ofloxacin occurred in U.S. wastewater treatment facilities at
213 about 80% detection frequency with concentrations ranging from 400-500 ng L⁻¹. Around 600
214 ng L⁻¹ of CPX in wastewater effluents in Spain was reported (Figure 2). In Sweden, reported
215 effluent ofloxacin concentration was 1,000 ng L⁻¹, whereas 7,600 ng L⁻¹ was the level found in
216 China. In all of these countries, hospital wastewater treatment facilities served as the primary
217 point source of FQs whereas other point sources are from sewage sludges, surface run-offs and
218 from soil, plants and manure.

219 An extensive study concerning the occurrence of antibiotics in a sewage treatment plant in
220 Qinghe, China, indicated that ofloxacin (1,287 ng L⁻¹) and norfloxacin (775 ng L⁻¹) were the
221 most prevalent drug species in the wastewater effluent [27]. The wastewater treatment process
222 was inefficient in removing all of the FQs; the final concentrations of ofloxacin and norfloxacin
223 in the final sludge were 1,140 and 610 ng mg⁻¹ respectively. Based on previous studies on the
224 occurrences of FQ in soil, water, sludge and manure in different countries and regions, the
225 antibiotics are mapped in Figure 2, in terms of the mean values of their occurrences in each
226 country. As reported by the World Health Organization (WHO), 63 out of 187 countries
227 (~34%) under their survey identified FQs in water bodies, mostly in wastewaters and sludge
228 systems (Table 1) [46–48]. In most areas, low concentrations of FQ antibiotics are undetectable
229 which adds strain to the environment with the consecutive accumulation of the pollutants at
230 unpredictable rates [49]. Although samples from those areas, especially in the developing
231 nation, did not contain parent FQ compounds, their transformed products could occur (due to

232 changes in the solution chemistry) and currently are not taken into account for toxicity
233 assessment and regulatory measures.

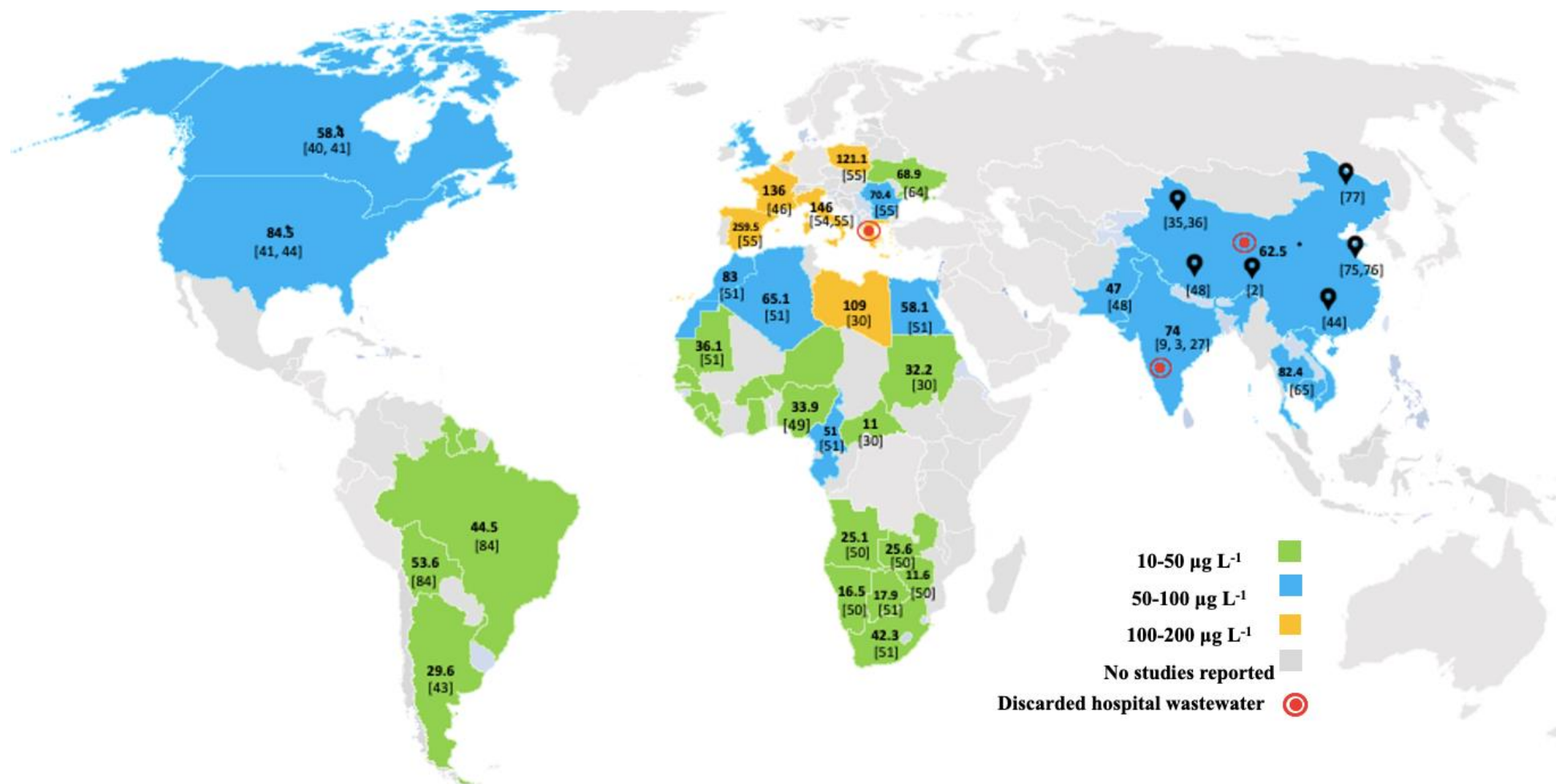


Table 1: Occurrence of FQ-based antibiotics with sources and concentrations

Concentrated Sample Sources	Class of quinolone	Study location	Maximum Concentration ($\mu\text{g L}^{-1}$ except noted below)	References
Sewage sludge	Ciprofloxacin	South Africa	0.12 (mg kg^{-1})	[50]
		South Africa	99.2 (mg kg^{-1})	[51]
		Italy	0.514 (mg kg^{-1})	[52,53]
	Ofloxacin	Beijing, China	0.336 (mg kg^{-1})	[27,28]
	Norfloxacin	Beijing, China	0.256 (mg kg^{-1})	[27]
	Gatifloxacin	Beijing, China	0.066 (mg kg^{-1})	[27]
	Ciprofloxacin	USA	40.81 (mg kg^{-1})	[54]
	Ofloxacin	USA	58.1 (mg kg^{-1})	[54]
Hospital wastewater	Ciprofloxacin	Ghana	15.733	[34]
			31,000	[55]
		Spain	13	[56]
	Norfloxacin	Taiwan, Australia, China	1.15- 6.06	[57,58]
	Ofloxacin	Hyderabad, India	160	[55,59]
		Spain	13	[56]
	Norfloxacin	Iraq	450	[60]
	Ofloxacin	Spain, Italy	8.77	[55,56,65]
Surface water	Ciprofloxacin	Ghana	1.168	[34]
	Enrofloxacin	China	4.24	[61]
	Nalidixic acid	South Africa	23	[51]
	Ciprofloxacin	South Africa	14	[51]
		South Africa	27.1	[51]
		New York	5.6	[62,63]
		Nigeria	0.9	[64]
	Ofloxacin	Spain, Italy	8.77	[55,56,65]
Run-off	Levofloxacin	Beijing, China	0.213	[66,67]
	Norfloxacin	Chongqing, China	0.0924	[67,68]
	Moxifloxacin	China	0.64	
	Ofloxacin		11.4	
	Ofloxacin	Vietnam	17.7	[69]

Soil, plants and manure	Norfloxacin	India	16.4	[9]
	Ciprofloxacin			
	Enrofloxacin			
	Ofloxacin	Taiwan	11.8	[66]
	Enrofloxacin	Vietnam	1.2	[70]
	Ciprofloxacin	China	29,590 $\mu\text{g kg}^{-1}$	[71,72]
		Japan	12 $\mu\text{g kg}^{-1}$	[72,73]
	Enrofloxacin	USA	46,700 $\mu\text{g kg}^{-1}$	[72,74]
	Norfloxacin		2,760 $\mu\text{g kg}^{-1}$	[63,75]
	Levofloxacin	China	5,530 $\mu\text{g kg}^{-1}$	[2,76]
			manure	
	Enrofloxacin	China	15 mg kg^{-1}	[62,77,78]
			chicken feces	
			33 mg kg^{-1} pig	[78]
			manure	
		Turkey	70 $\mu\text{g kg}^{-1}$ cattle	[78,79]
			manure	
	Ofloxacin	China	16 $\mu\text{g kg}^{-1}$	[76]
			livestock farms	
	Norfloxacin		4.4 $\mu\text{g kg}^{-1}$	[40]
			2.8 ng g^{-1} carrot	[2,41]
			21.8 $\mu\text{g kg}^{-1}$	
			cabbage	
	Ofloxacin		3.60 g g^{-1} celery	

239

240 2.2.3. Persistence of FQs in the environment

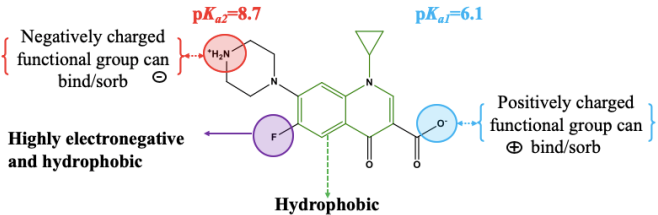
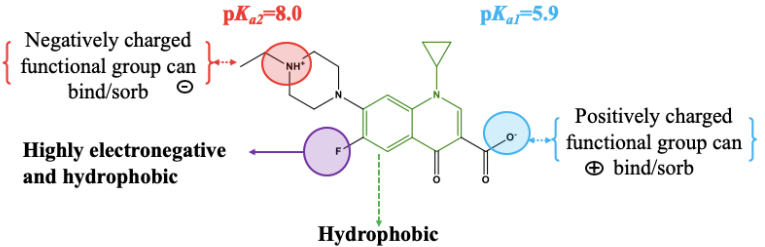
241 The persistence of FQ in the environment is of high significance owing to its extremely slow
242 biotic and abiotic degradation in soil and water. The degradation is mainly governed by the pH
243 of the soil and water matrices. Various functional groups in FQs result in high solubility of FQ
244 species over a wide environmental pH range. For example, FQs contain more than one
245 basic/acidic groups (e.g. -OH, -NH₂ and -COOH) that can persist in soil and water via existing
246 in both charged species as tabulated in Table 2. Transformed species and acidic/basic sites of
247 some predominantly found FQs are also tabulated. Transformation of FQs with the alterations
248 in solution pH makes these antibiotics equally prevalent than their parent counterpart when
249 present in the environment viz., in surface water and groundwater [7,26,43,80].

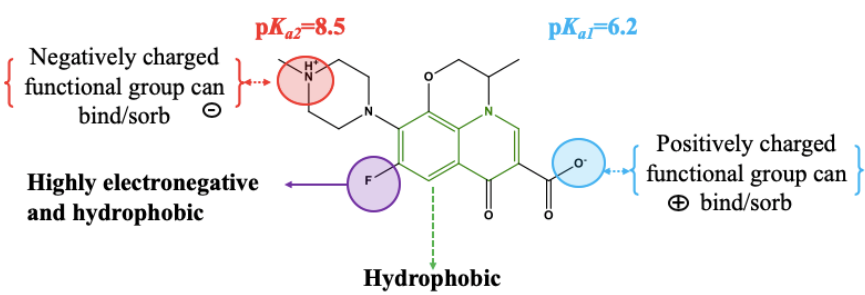
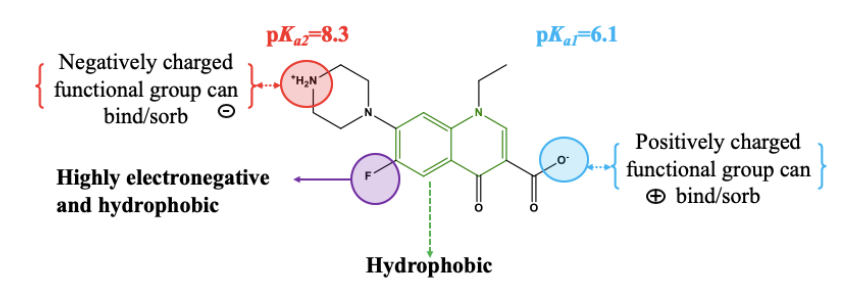
Numerous studies have demonstrated that FQs are not readily biodegradable in the environment [9,29,81]. EFX and CPX, which are the most prominent FQ antibiotics, can get slowly degraded by brown-rot fungi in the environment. Manganese oxide in the soil facilitates FQ degradation abiotically by providing an interface for the oxidation reactions [82,83]. The piperazine moiety of FQ can be transformed through differently charged species through the process of dealkylation and hydroxylation from the hydrated media. This binds on environmental particles such as soil and sediments and thus, the FQ ring remains intact and the active ingredient remains persistent in the soil [84].

Accumulation of FQs in sewage sludge is also of particular concern because of the dynamic physicochemical nature of the sludge and its further application to soil as a fertilizer [31]. Traces of FQs upon accumulation in the closed sludge system ultimately leads to direct exposure to the soil environment. [30–32,85]. With very low concentrations of FQ antibiotics present in the closed system over a long period, bacteria develop resistance against these compounds. For example, norfloxacin in the sludge exhibited a residence time of about 4-8 days [9].

Numerous adsorption studies over the past few years have been based on the removal of antibiotics by non-engineered and engineered carbon-based adsorbents for enhanced sorption for mitigating a wider range of emerging pollutants. However, details of the mechanistic pathways of adsorbents for FQ antibiotic removal are limited. Thus, a dedicated review on adsorptive removal of FQ-antibiotics necessitates for the identification of merits and demerits of each adsorbents based on performance through revisiting the literatures systematically and at a critical approach.

Table 2: Physicochemical characteristics of commonly found FQs with their transformed species

Physicochemical properties	Structures and zwitterionic state	References
Ciprofloxacin $C_{17}H_{18}FN_3O_3$ Molecular weight: 331.35 g mol ⁻¹ Solubility: 3.46 mg mL ⁻¹ Vapor pressure: 1.3x10 ⁻¹³ mm Hg Log K_{ow}: -1.70		[25,86]
Enrofloxacin $C_{19}H_{22}FN_3O_3$ Molecular weight: 359.40 g mol ⁻¹ Solubility: 0.146 mg mL ⁻¹ Vapor pressure: 1.89x10 ⁻¹³ mm Hg Log K_{ow}: 3.48		[44,86,87]

<p>Ofloxacin</p> <p>C₁₈H₂₀FN₃O₄</p> <p>Molecular weight: 361.37 g mol⁻¹</p> <p>Solubility: 95.4 mg mL⁻¹</p> <p>Vapor pressure: 9.8x10⁻¹³ mm Hg</p> <p>Log K_{ow}: 2.4</p>		<p>[86,88]</p>
<p>Norfloxacin</p> <p>C₁₆H₁₈FN₃O₃</p> <p>Molecular weight: 359.396 g mol⁻¹</p> <p>Solubility: 161 mg mL⁻¹</p> <p>Vapor pressure: 1.6 1.89x10⁻¹³ mm Hg</p> <p>Log K_{ow}: -2.0</p>		<p>[86,89]</p>

3. Adsorption of FQs by carbon-based, tailored and other material adsorbent

Tested FQ adsorbents most often include activated carbon, graphene, biochar, carbon nanotubes (CNTs), iron-based adsorbents, and clay-based adsorbents. However, knowledge on the functional relationship between these commonly studied adsorbents and the actual environmental applications is scarce especially in terms of their distinct performances.

The performance of an adsorbent is generally assessed by the equilibrium or maximum adsorption capacity. Since, the experimental conditions such as initial adsorbate concentration, the dosage of adsorbents used, and the contact time between the adsorbate and adsorbent are varied widely among published studies, it is technically more apt to use partition coefficient for the comparison among adsorbent performances. Moreover, partition coefficient gives a normalized value derived from both the equilibrium adsorbate concentration and adsorption capacity, and thus provides an actual performance of the adsorbent that further enables fair comparisons among adsorbents, despite a wide range of initial experimental conditions [90,91]. The partition coefficient is derived from the ratio of the maximum adsorption capacity to the equilibrium adsorbate concentration in the media [90](Eq. 1).

$$\text{Partition coefficient} = \frac{q_e}{C_e} \quad (1)$$

where, q_e is the equilibrium adsorption capacity, and C_e is the equilibrium adsorbate concentration.

Studies on the adsorption of FQ in aqueous solutions typically examine the adsorption kinetics and isotherms to understand the performance of the adsorbent. The most widely used kinetic model has been the pseudo second-order model, which satisfies chemisorption mechanisms for FQ uptake by various adsorbents. Both Langmuir and Freundlich isotherm models were reported to fit FQ adsorption data (Table 3). Multi-layer adsorption (Freundlich model) of FQ appeared to be the more frequently reported mechanism than the mono-layer adsorption

(Langmuir model) mechanism. The sections below assess the performance of various tailored and natural adsorbents in relation to their physicochemical characteristics and prevailing adsorbate concentrations through the use of partition coefficients.

3.1. Carbon-based adsorbents for FQs removal

Several carbon-based adsorbents have been assessed for the removal of FQs from aqueous media. Adsorptive removal of FQs onto carbon-based adsorbents largely depends on the surface porosity of the adsorbent, tunable chemistry of functional groups on the adsorbents, the specific surface area and dosage of the adsorbent. Prominent interactions for FQ removal by these adsorbents include surface/pore diffusion, electrostatic interaction, van der Waals forces, hydrogen bonding and π - π electron donor-acceptor (EDA) interactions [21,92,93]. Based on the source of carbon precursors and structure of the final products, carbon-based adsorbents can be classified into four groups: activated carbon (AC), biochar, carbon nanotubes (CNTs), graphene, and graphene oxides.

3.1.1. Activated carbon

Activated carbon (AC) is used in a wide range of applications including water and wastewater treatment. It has an amorphous structure with a highly porous interior and large surface area. The pore structures are tunable through various surface modifications, and that is why AC has been widely used for the remediation of antibiotics in wastewater [15,94]. Owing to a planar molecular configuration, FQ antibiotics can enter into the pores of AC and move sideways reaching a high number of adsorptive sites [95].

Activated carbons, developed from different precursors, have been assessed for their removal capacities of FQ antibiotics. AC derived from root-based biomass (e.g., *Eichhornia crassipes*) showed high adsorptive removal of CPX (145 mg g⁻¹) and norfloxacin (NFX) (135.1 mg g⁻¹)

[96]. Adsorption equilibrium was reached in 8 h obeying the pseudo-first and pseudo-second-order kinetics for CPX and NFX, respectively. [96]. Similarly, CPX showed a strong affinity to a commercial-grade AC under acidic solution pH [97]. Due to the speciation of CPX, negatively charged carboxylic groups co-exist and the surface charge of activated carbon, which is positive at acidic pHs, provided a high CPX removal capacity of 131.14 mg g⁻¹. Kinetics and isotherm experiments indicated significant removal of both CPX and NFX by commercial-grade AC [98]. Analytical grade AC offered favorable adsorption for CPX based on a partition coefficient of 12.7 [99]. Although the long-root *Eichhornia crassipes* AC had the highest surface area, its performance for the removal of ciprofloxacin and norfloxacin was found to be the lowest, based on the partition coefficient [96] (Table 3).

The surface of AC contains carboxylic acid functional groups that are negatively charged at pH > pHPZC, and thus, cationic FQ moiety can adsorb with ease on the negatively charged AC. Studies with AC showed chemisorption interactions with FQ. For example, Chowdhury et al. (2019) studied the efficacy of AC derived from industrial paper mill sludge for the sorption of enrofloxacin [100]. The adsorption process was exothermic in nature, and followed the Langmuir isotherm model and pseudo-second-order kinetic model, both suggesting chemical adsorption. The adsorption of FQ on AC could also occur on the outer surface via electrostatic forces. Ciprofloxacin, danofloxacin, and enrofloxacin interact with the AC electrostatically based on the pH of the ambient environment ranging between 6.09 and 9.43 of pK_a (Table 3).

Adsorption of FQ on AC takes place at a slightly acidic pH (in the range of 5-7) with the interaction of cationic and zwitterionic species of FQs in aqueous media. Interestingly, as reported by Kong et al. (2017) [101], with the increase in the initial concentration of OFX, the adsorption was favorable during the initial loading of the adsorbate on the adsorbent as it attained equilibrium at a much lower concentration of OFX [101]. In another study, a lower

initial concentration showed favorable adsorption and reached a saturation up to equilibrium concentration of 14 mg L^{-1} for the commercial-grade AC (NC01-125) for the removal of CPX with an optimal adsorption capacity of 230 mg g^{-1} [102]. This is further supported by the partition coefficient (PC) values obtained for both the studies; 0.717 [101] and 1.179 L g^{-1} [102], indicating that only the larger surface area does not facilitate the performance of the adsorbents. Despite the amorphous nature of AC and the lack of diverse functional groups for the uptake of antibiotics, adsorbing FQ antibiotics is scarce. However, as reported by Xiang et al. (2019), AC with an enhanced specific surface area ($487 \text{ m}^2 \text{ g}^{-1}$) shows the maximum adsorption capacity for CPX adsorption. Comparatively, the initial conditions for the adsorption studies are not consistent with the rest of the studies reported in the literature [92]. Therefore, systematic studies are needed, in which the initial loading concentration remains the same for one kind of FQ, thus enabling the adsorption affinity study clearer, which is difficult to achieve otherwise, with the other FQ antibiotics. Figure 3 demonstrates the mechanisms involved for the removal of FQ antibiotics by carbon-based adsorbents. Ofloxacin, norfloxacin and ciprofloxacin were used to explain the predominant mechanism.

Regenerability is a crucial property of an adsorbent from an economical point of view and enables recovery of adsorbents for reuse. Solvent extraction, microwave radiation, chemical and catalytic decomposition are some of the regeneration processes, apart from thermal treatment. Thermal treatment with an inert atmosphere is the usual procedure to recover the adsorbent surface to improve the porosity of the adsorbents. Almost 60% of the adsorbent were restored through thermal regeneration after two saturation-regeneration cycles. Destruction of the porosity and the textural alterations in the AC were observed when heated to more than 600°C , whereas optimum temperature was maintained between 400 and 600°C where the surface remained intact up to two cycles [10,103]. Elution studies were conducted for norfloxacin and ciprofloxacin using ethanol, methanol and acetone for adsorption-desorption cycles and

370 indicated that after five eluents cycles, the performance was high and the acetone exhibited the
371 highest performance efficiency compared to ethanol and methanol [89,104]. About 80% of
372 adsorption capacity can be maintained with five consecutive regeneration cycles. There are
373 only a few studies that explain the desorption mechanism and thus further understanding of the
374 desorption mechanism through thermal regeneration and chemically-assisted regeneration,
375 needs to be better identified through the use of the efficient desorption agent [105–107].

376 **Table 3: FQ adsorption performances, characteristics, mechanisms of activated carbon-based adsorbents with and without composite**
377 **material(s).**

Type	Composite	Quinolone	pH _{PZC}	Optimal pH	Q _{max} (mg g ⁻¹)	PC (L g ⁻¹)	Specific Surface Area (m ² g ⁻¹)	Best fitted model	Mechanism	References
Waste tires AC	Polyacrylonitrile nanofibers. and activation via hydrogen peroxide	CPX EFX DFX	6.7	6.5	93 99 112	0.338 0.360 0.410	-	-	Electrostatic interaction	[104]
Long-root <i>Eichhornia crassipes</i> AC	Pristine	CPX NFX	3.3	4.2	145 135.1	3.563	1525.62	Langmuir isotherm and pseudo-first, pseudo-second order kinetic model	electrostatic interaction, hydrogen-bond, EDA interaction	[96]
Paper sludge AC	Pristine	EFX	5.7	5.4	44	0.247	-	Langmuir isotherm	Monolayer interactions	[100]
Luffa fibers AC	Pristine activation via H ₃ PO ₄	OFX	4.3	6	132	0.717	-	-	Freundlich isotherm Pseudo-second order kinetics	[101]
AC (commercial grade)	Pristine Activation via KOH	CPX NFX	5.9	4.7	-	-	852	-	Pseudo-second order and intraparticle diffusion model with Langmuir isotherm	[108]
	Pristine Activation via KOH	CPX NFX	6.5	5	131.14 167	0.661 0.843	-	-		[98]
AC (NC01-125)	Pristine	CPX	-	5	230	1.179	1231	Langmuir Freundlich isotherm	Electrostatic interactions	[102]
	Pristine	CPX EFX	-	7	140	12.7	-	Freundlich isotherm	Hydrophilic interaction with π - π interactions	[99]

AC (analytical grade)								Pseudo-first and second order kinetic models		
	Pristine Activation via KOH	CPX	-	6.2	0.26 mmol g ⁻¹	-	1075	Freundlich Langmuir isotherm; pseudo- first and pseudo- second order models	π - π electron donor- accepter	[109]
	Pristine	CPX	-	5	69.4	8.6	990	Pseudo-second order kinetics model	Electrostatic interactions	[110]

378

379 AC: Activated carbon, CPX: Ciprofloxacin, EFX: Enrofloxacin, NFX: Norfloxacin, OFX: Ofloxacin, DFX: Danofloxacin

3.1.2. Biochar

A significant number of studies have focused on removing FQs by biochar (BC). The application of BC for the removal of FQ-based antibiotics has been proven challenging because of FQ speciation in the environmental matrices [111]. For the majority of adsorbents used for FQ adsorption, adsorption affinity is favorable within a limited range of solution pH and/or the adsorption decreases with the increase in the negative surfaces of the sorbents with increasing pH. These shortcomings can be resolved by applying BC as a multi-functionality sorbent [112,113]. A thermally synthesized reed straw BC composite with hematite and pyrite was able to remove NFX with the adsorption capacity of 345 mg g^{-1} , which is 2-fold higher than that of the pristine BC suggesting a strong multi-layer adsorptive removal with a good fit with the Freundlich model. Favorable removal was observed at pH 6 to 7 with the pH_{PZC} at 4 [114]. Similar pH dependency was observed for BC derived from camphor leaves with maximum ciprofloxacin adsorption at pH 5.5-6.0 with pH_{PZC} at 3.5 [115]. Table 4 summarizes the adsorptive removal of FQ by BC generated from different sources and under different pyrolyzing conditions.

Biochar, ideally, has variable adsorption capacity for organic pollutants because of its heterogeneity in functional groups on the surface. Multi-layer adsorption with electrostatic interactions of hematite-BC composite resulted in NFX adsorption capacity of 325 mg g^{-1} and a PC value of 11.61 L g^{-1} [17]. BC derived from cattails containing porous carbon sheets for the remediation of LVX was studied by Yang et al. (2020) [116]. The maximum adsorption capacity was observed for cattail BC produced from the highest temperature (650°C) at 754.12 mg g^{-1} [116]. Chemically stable municipal solid waste BC had a maximum CPX adsorption capacity of 286.6 mg g^{-1} , which was about 6-fold higher than those of other BC adsorbents with comparable PCs of around 2.0 L g^{-1} .

Biochar with its diverse functionalities contains oxygen-containing groups such as the carboxyl (-COOH), hydroxyl (-OH), and arene (such as benzene-rings) groups, which are vital for FQ uptake [117–119]. At increased pyrolysis temperatures (up to 500 °C), aromaticity increases accompanied by loss of hydroxyl and carboxyl containing groups. This enables the presence of electron donor and electron acceptor groups on the adsorbent surface, further interacting with the like portions of the FQ antibiotics [120] (Figure 3).

Application of BC produced from vinasse waste for the quinolone decontamination is yet another viable approach. Vinasse waste was treated with co-precipitated Fe and Mn and then pyrolyzed, forming manganese ferrite modified biochar (FMB), which was examined for the adsorption of CPX and pefloxacin (PFX) [121]. At neutral pH, the highest adsorption capacity was 146 mg g⁻¹ which might be attributed to the hydrophobic nature of the adsorbent at the near-neutral pH conditions, and this, in turn, showed a positive effect on the decontamination of PFX and CPX [18,122].

In another study, the maximum CPX adsorption capacity of cassava-based BC (produced at 650 °C), was 449.40 mg g⁻¹. However, the adsorption capacity of the same BC produced at a lower pyrolysis temperature (400 °C) decreased to 2- fold [115]. More interestingly, Hu et al. (2019) demonstrated that the removal of CPX from aqueous solution was more efficient with the ZnO-BC composite than with the original BC derived from camphor leaves, prepared at the same temperature (500 °C). Moreover, a maximum CPX adsorption capacity (238 mg g⁻¹) was reported for BC generated from used tea leaves. The best fits were obtained using Langmuir isotherm and pseudo-second-order kinetic model, suggesting the involvements of monolayer and chemisorption interactions [117]. Modified BC produced at a higher temperature (> 500 °C) tends to offer maximum organic removal. Thus, for choosing the appropriate adsorbent for remediating different FQ, extensive studies needs to be carried out.

428 Shengze et al. (2016) investigated the desorption rates for levofloxacin from rice husk and
429 wood chip BC (previously used for levofloxacin adsorption) in batch experiments. The result
430 obtained in this study showed that levofloxacin remained on the BC through intra-particle
431 diffusion for higher pyrolysis temperature of BC [123]. Peng et al. (2018) studied the
432 desorption behavior of BC derived from Cassava produced over a wide temperature range of
433 350-650 °C and higher desorption rates were observed for BC at higher pyrolysis temperatures
434 (650 °C) due to the higher specific surface area and larger micro-pore volume [124].
435 Desorption facilitates during the first few time intervals when the adsorbates are loaded and
436 the behavior varies when pyrolysis temperatures are altered. It is due to these contributory
437 factors that the solute destabilizes the adsorbent surface and elutes faster, thereby, giving higher
438 regeneration capacity. Moreover, desorption is inversely proportional to the specific surface
439 area, i.e., more regeneration cycle for the same BC having lesser specific surface area.
440 Therefore, while selecting an appropriate BC for remediating particular FQ from water,
441 pyrolysis temperature must be considered for BC synthesis. Thus, batch adsorption studies
442 need to be further extended for each FQ antibiotics onto varied BC-types originating from
443 different sources and pyrolysis temperatures at which BC is being synthesized.

444 **Table 4: FQ adsorption performances, characteristics, mechanisms of biochar-adsorbents with and without composite material(s)**

Biochar type	Pyrolysis conditions	Composite	FQ	pH _{PZC}	Optimal pH	Q _{max} (mg g ⁻¹)	Specific Surface area (m ² g ⁻¹)	Best fitted model	Mechanisms postulated	PC (L g ⁻¹)	References
Reed Straw	500 °C 5 hours	Hematite and pyrite	NFX	4	7	325	160 55	Freundlich isotherm	Multi-layer with electrostatic interactions	11.61	[114]
Rice straw		Molybdenum disulfide (MoS ₂)	CPX	3.4	6-8	52.75	610.4	Freundlich isotherm and pseudo-second order	Chemisorption and π - π electron donor interactions	4.34	[125]
Sugarcane bagasse and ore mixed	800 °C	Ferromanganese	LVX	-	5	212		Freundlich isotherm and pseudo-second order interactions	π - π stacking interactions	5.3	[121]
Potato leave and stem	500 °C 6 hours	Magnetic composite with humic acid	CPX	-	7	12	98 (pristine) 48 (magnetic BC) 22 (humic acid)	Langmuir isotherm with pseudo-second order kinetics		0.5 0.33 0.416	[126]
			NFX			8					
			EFX			10					
Camphor leaves	500 °C 650 °C 800 °C 2 hours	Magnetic ZnO composite	CPX	3.4	5.5	500	915	Langmuir isotherm and pseudo-second - order kinetic	π - π stacking interactions with electrostatic interactions	22.7	[115]
Pomelo grapefruit	450 °C 30 minutes	Chitosan and hydrogel beads	CPX			76		Langmuir isotherm and Pseudo-second	Monolayer heterogenic and hydrogen bonding	4.22	[127]

								order and intra-particle kinetics			
Cassava	500 °C 1 hour	Pristine with KOH activation	NFX	3	4-7	287	128	Langmuir isotherm and pseudo-second order	π - π EDA interactions	12.58	[128]
Municipal solid waste	450 °C 30 min	Bentonite-biochar composite (450 °C pyrolyzed municipal solid waste)	CPX	5.7	6	286.6	7	Elovich kinetics model and hills isotherm	Hydrogen bonds with π - π electron donor interactions and electrostatic attractions	2.01	[17]
Used tea leaves	550 °C for 30 min each	Pristine	CPX	3.05	6	238		Langmuir isotherm with pseudo-second order	π - π interactions	15.84	[116]
Cassava	700 °C	Pristine	OFX	-	6	-			Freundlich isotherm	heterogeneous adsorption	[124]
Cattail	900 °C (max adsorption) with acid activation	Pristine	LVX	9.01	5	754	2240		π - π EDA interaction, pore filling, electrostatic interactions	30.2	[18]
Vinasse	800 °C	Activated composited with co-precipitated Fe and Mn	PFX CFX	7.97 8.31	5	253 133	94.943	Pseudo-second-order kinetics and Freundlich model	Magnetic and electrostatic interactions	14.7 10.6	[18]

3.1.3. Graphene-based adsorbents

Graphene is a highly electron-rich and hydrophobic adsorbent, and has a large surface area, making it appropriate for remediating antibiotics from water [129]. Oxygen-containing functional groups on graphene including hydroxyl, carboxyl, and carbonyl-groups have proven to be a crucial characteristic for organic contaminant removal from aqueous media [92].

Graphene-oxide assembled with chitin was tested for CPX adsorption. Electrostatic attraction and mono-layer interaction between CPX and graphene-oxide, were the predominant interaction along with the surface functional groups of composites which ultimately contributed to a higher PC of 23.78 L g⁻¹ and at optimum adsorption capacity of 282 mg g⁻¹. Furthermore, the removal of CPX from aqueous media by pristine graphene oxide, synthesized by a co-precipitation method, was experimented by Chen et al. (2015) [130]. An adsorption capacity of 379 mg g⁻¹ with a PC of 44.27 L g⁻¹ was obtained. The electrostatic attraction was considered as the dominating mechanism with a strong dependency on the solution pH and the speciation.

CPX adsorption on graphene oxide was high at pH 2 with the carboxylic and amine groups protonated thereby attracting CPX to the graphene oxide surface through hydrogen bonds [131,132]. The effect of ionic strength on CPX adsorption onto graphene oxide was studied by Chen et al. (2015) [130]. Both CaCl₂ and NaCl have been studied and it was found that as the ionic strength increased, the sorption of CPX declined further confirming the electrostatic attraction mechanism. The higher concentration of Ca²⁺ in the solution also suppressed the CPX sorption, which was explained through the complexation of Ca²⁺ with the GO surface, thereby declining the viable sorption sites for CPX [130,133]. Among different types of graphene oxide studied, pristine graphene oxide showed the highest efficiency for the removal of CPX and an adsorption capacity of 379 mg g⁻¹ and a PC value of 44.27 L g⁻¹ were reported

(Table 5). As summarized in Table 5, a significantly high surface area for magnetic modification of graphene oxide was observed compared to its pristine counterpart and was more suitable for the removal of CPX. Owing to the crystalline nature of graphene (Figure 3) and significantly higher specific surface area than BC and AC, there have been studies on its potential as an adsorbent for FQs [134,135]. For these studies, details on surface charge (pH_{PZC}) were not enough to elucidate the mechanisms that accounted for the high adsorption. Thus, further comparison between different graphene-based adsorbents and their modifications on the performances for the removal of FQ antibiotics was not possible. Graphene offers a rich structural distinction compared with other carbon-based adsorbents and a tunable pore, thus enabling the modification and uptake of FQs, much easier. Yet conclusive information on the mechanism of adsorption with varied graphene structures and FQ antibiotics is scarce and thus, more in-depth studies are needed.

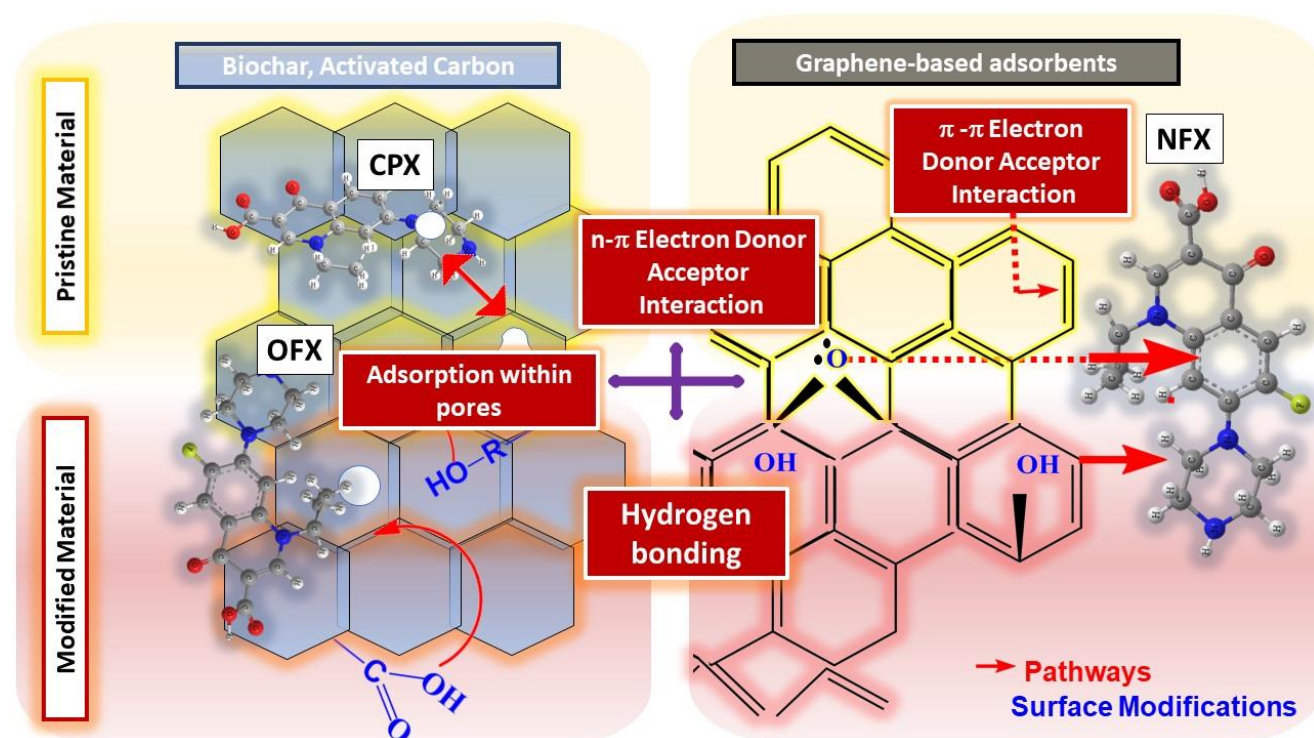


Figure 3: Predominant interactions of FQ-antibiotics with biochar, activated carbon and graphene-based adsorbents

485 **Table 5: FQ adsorption performances, characteristics, mechanisms of graphene- based adsorbents and composite material(s)**

Graphene-based	Modification	Quinolone	pH _{PZC}	Optimal pH	Q _{max} (mg g ⁻¹)	PC (L g ⁻¹)	Specific Surface area (m ² g ⁻¹)	Best fitted model	Mechanisms postulated	References
Graphene oxide	Chitin	CPX	5.5	4	282	23.78	-	Langmuir and Freundlich isotherm	Monolayer interactions and Electrostatic interaction, hydrophobic interaction via a salting out effect.	[136]
	Unmodified	LVX CPX	-	7	409	-	-	Langmuir isotherm	attractive electrostatic and π - π interactions form functional groups	[137]
	Magnetic chitosan grafted Unmodified	CPX	-	5	282.9 162.3	12.83 6.783	1685.7 -	Langmuir and Freundlich isotherm with second order kinetics	Electrostatic interaction	[138]
	Sodium alginate	CPX	5.6	4	86	9.05	92	Freundlich and Langmuir isotherm with pseudo-first order	Monolayers adsorption with homogenous sites	[139]
	Unmodified	CPX	-	5 9	379	44.27	-	Freundlich and Langmuir isotherm with pseudo-second order kinetics	Electrostatic interaction	[130]

486

487 CPX: Ciprofloxacin, EFX: enrofloxacin, NFX: Norfloxacin, OFX: Ofloxacin

3.1.4. Carbon nanotubes

Applications of CNTs for the adsorption of FQ antibiotics have also been examined. A study by Avcı et al. (2020) on the adsorption of CPX hydrochloride by CNTs indicated an optimum adsorption capacity of 1.75 mg g^{-1} at an initial concentration of 4 mg L^{-1} and removal of about 90% [140]. Heterogenous surficial adsorption was suggested by the Freundlich model being a good fit, whereas an agreement between the pseudo-second-order model and kinetic data indicated a chemisorption mechanism [19,140]. A study on CPX adsorption onto CNTs indicated that the double-walled CNTs provided a faster adsorption rate [141] and a higher PC, 46.36 L g^{-1} , compared to single-walled CNTs with a PC of 16.56 L g^{-1} [142] (Table 6). The electronegative entities in CPX, ofloxacin (OFX) and norfloxacin (NFX) compete with the electron-deficient entity of CNTs and enhance the removal of these FQs in aqueous media.

Solution pH influenced the FQ removal and in the case of CNTs with a consistently charged surface, FQ adsorption was more prominent from slightly acidic pH to neutral pH via electrostatic attraction and EDA interactions. For norfloxacin, single-walled CNTs (SWCNTs) exhibited the highest performance (PC value of 46.65 L g^{-1}) as shown in Table 6. Hydrolyzed multi-walled CNTs (MWCNTs) were tested for OFX and NFX adsorption and the results revealed that both were adsorbed on the CNTs at a similar rate and isotherm data fitted both Langmuir and Freundlich models with EDA as the main adsorption mechanism [143]. However, practical applications of CNTs for the remediation of FQ antibiotics remain challenging because of their higher manufacturing costs and the consequences it pertains due to its high dispersion in different aqueous media [144]. Hence, future research is needed to elucidate mechanisms for its adsorption.

The agglomeration of CNTs in aqueous solutions is one of the limitations which restricts its usage for water and wastewater treatment [145,146]. This causes a reduction in the adsorption

capacity due to the hydrophobic behavior of the CNTs. Several studies have proven that surfactants can help the dispersion of CNTs to aggregate in the solution producing a stabilized suspension and with the help of sonication, CPX can easily be adsorbed on the CNTs. Thus, surfactants with sonication induced adsorption of the FQ antibiotics on CNTs generate active adsorption sites available for the antibiotics. The influence on the adsorption capacity by the surface charge of the CNTs has been studied further by inducing anionic and cationic-based surfactants in the initial solution of the CNTs [144]. The removal of FQ type antibiotics by CNTs is mostly dependent on the speciation of the antibiotics at varying pH, implying the importance of their sorption onto the charged CNTs through electrostatic binding. Overall, CNTs adsorb FQ-based antibiotics through micropore filling and π - π electron donor-acceptor complexes as predominant interactions. Surface bonding with polar entities on the FQ molecule also recurs, with the interchangeable charges on the CNT surface varying with pH. This kind of interchangeable charge-based interaction is via hydrophobic or electrostatic interactions [92,147]. Few modified CNTs showed close to 90% NFX removal, for example, hydroxylation-modification of SWCNTs enhanced adsorption capacity as compared to the pristine SWCNTs [148]. Figure 4 depicts the treatments and modification of the CNTs with the predominant mechanisms demonstrated.

Another significant observation from the CNTs-based studies for the removal of FQs is that the feed concentrations used in the synthetic experiments ($10\text{--}20\text{ mg L}^{-1}$) [143] are much higher than the environmentally occurring concentrations (as low as ng L^{-1} to $\mu\text{g L}^{-1}$). Based on the mentioned studies, higher concentrations are taken in the synthetic experiments to compensate for any variations of concentration in the environment concentration. However, there is an immediate need for the case of mitigating FQ from natural water where the concentrations of FQs are comparatively lower than that of a synthetic solution used in the laboratory, to further optimize the dosage of CNTs for actual contaminated water. Therefore, more in-depth studies

are suggested for the successful practical application of CNTs for FQ removal. Moreover, the excruciating high cost of CNTs and the capital cost to scale up CNTs-based systems for further pilot research and demonstration cannot be overlooked as it requires much higher dosage [149].

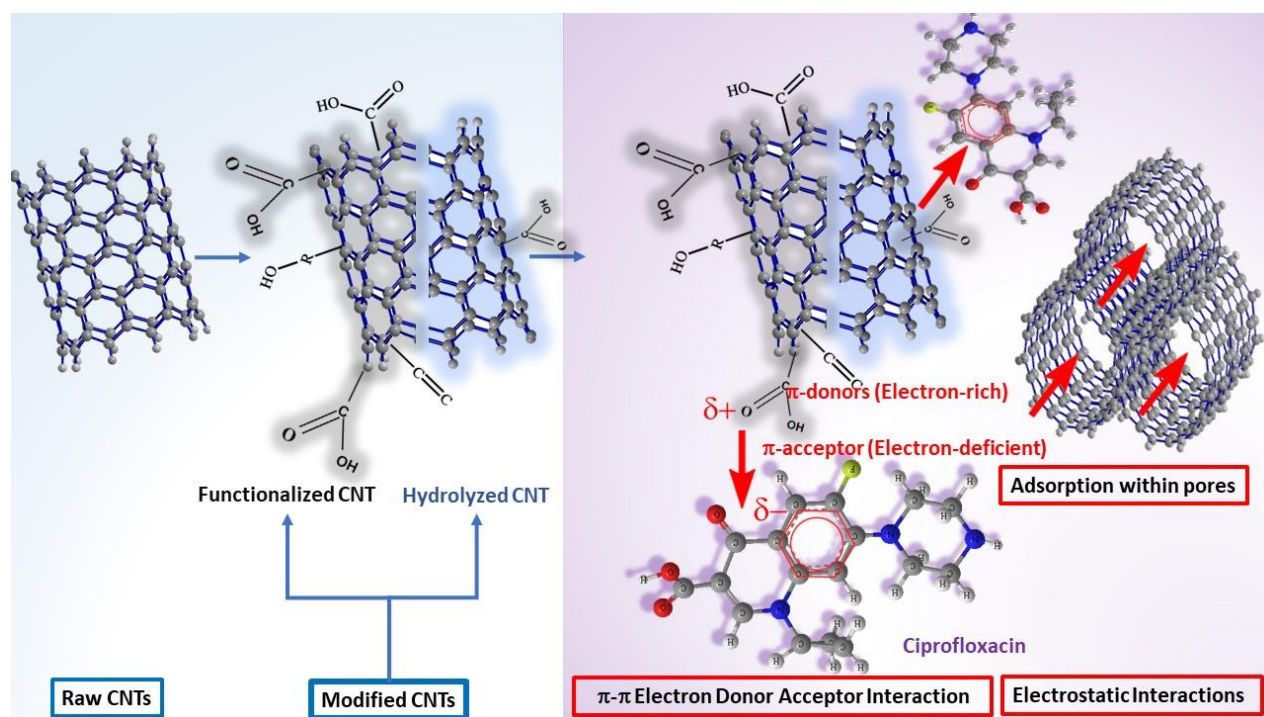


Figure 4: Predominant interactions of FQ-antibiotics with carbon nanotubes

542

Table 6: FQ adsorption performances, characteristics, mechanisms of pristine and modified carbon nanotubes-based adsorbents

Type	Modification	Quinolone	Optimal pH	Q_m (mg g ⁻¹)	PC (L g ⁻¹)	Mechanisms postulated	References
SWCNT	Pristine	CPX	7	724	39.2	Hydrophobic π - π interactions	[141]
Double walled CNTs	Pristine		4	689	46.36		
MWCNT	Pristine		4-7	475	25.51		
MWCNT	Hydrolyzed	OFX NFX	7	15.3 14.5	-	Langmuir and Freundlich isotherm π - π EDA interaction	[143]
MWCNT	Pristine	CPX	5	1.74	0.217	Freundlich isotherm and pseudo-second order kinetics chemisorption model	[140]
SWCNT	Graphene oxide, hydrogels and alginate)	CPX	5.4	181	46.56	π - π EDA interaction	[142]
SWCNT	Hydroxylated	NFX	6.7	181	22.62	π - π EDA interactions	[150]
SWCNT	Carbolized	CPX	7	-	-	Freundlich isotherm model. Electrostatic dictating hydrophobic EDA interaction	[151]

543

544

545 CNT: Carbon nanotube, CPX: Ciprofloxacin, EFX: enrofloxacin, NFX: Norfloxacin, OFX: Ofloxacin

3.2. Adsorptive removal of FQ antibiotic by clay and tailored adsorbents

Many researchers have used other non-carbon-based adsorbents for FQ removal from water, including magnetic nano-sorbents [114], zeolite-based adsorbents [152,153] and metal-based composite sorbent materials. The composition, shape and size of the nano-sorbents affect the mechanisms for antibiotic adsorption [154]. The electrostatic effect, hydrogen bonding, and coordination and hydrophobic effects are some of the significant interactions which have been reported between nano-based materials and antibiotics [155,156].

3.2.1. Clay adsorbents

High porosity and crystallinity are the intrinsic properties of clays that make them suitable sorbents for mitigating antibiotics in aqueous media [157,158]. Montmorillonite (MMT) and kaolinite are two clay minerals that behave differently with various contaminants due to differences in their properties, including surface charge and specific surface area. Furthermore, these clay minerals are 20 times more affordable in cost than commercially available activated carbons [132,159].

Montmorillonite, which is a smectite type swelling clay mineral, has high cation exchange capacity, and high contaminant adsorption capacity [160]. Maximum LVX adsorption on montmorillonite occurred at pH 7 at which the zwitterionic form of LVX predominated; however, when pH was greater than 7, the adsorption declined due to repulsive forces between the adsorbate and adsorbent [161,162]. The infrared spectrum of the used adsorbent indicated carboxylic groups of the antibiotic interacting with the metal ions present in the clay mineral. The maximum LVX adsorption capacity was 57 mg g⁻¹ [162]. Higher maximum CPX adsorption capacity (128 mg g⁻¹) [163] was reported for MMT compared to kaolinite (14 mg g⁻¹) [97] and the adsorption followed the pseudo-second-order kinetics, suggesting the

involvement of multilayer adsorption (Table 7). Details presented in the above studies were not enough for the calculation of the partition coefficient in order to compare the performance of different clay-based adsorbents.

Physical adsorption of both neutral and anionic species of FQs is favorable when the cation concentration in the solution increases [162] (Table 7). Solution pH also governs the adsorption as it dictates the charge of the FQs and the clay minerals. In previous studies, the optimal pH for FQ adsorption on clay minerals was at the ambient environmental pH (~5-7) [162,164]. Si-OH and Al-OH are distinct features on the exposed edges of tetrahedral and octahedral sheets of clay minerals (Figure 5). The interaction of FQ-based antibiotics with these hydroxyl groups is least understood because the charge characteristic of these surface groups can widely vary depending on the pH values of the surrounding media. This suggests a further need for research to investigate the potential of clay minerals for the removal of FQ and to test the plausibility of using them as composite materials via incorporating with bio-based or carbon-based materials. A scheme showing the governing mechanisms for the adsorption of FQ on clay minerals is presented in Figure 5.

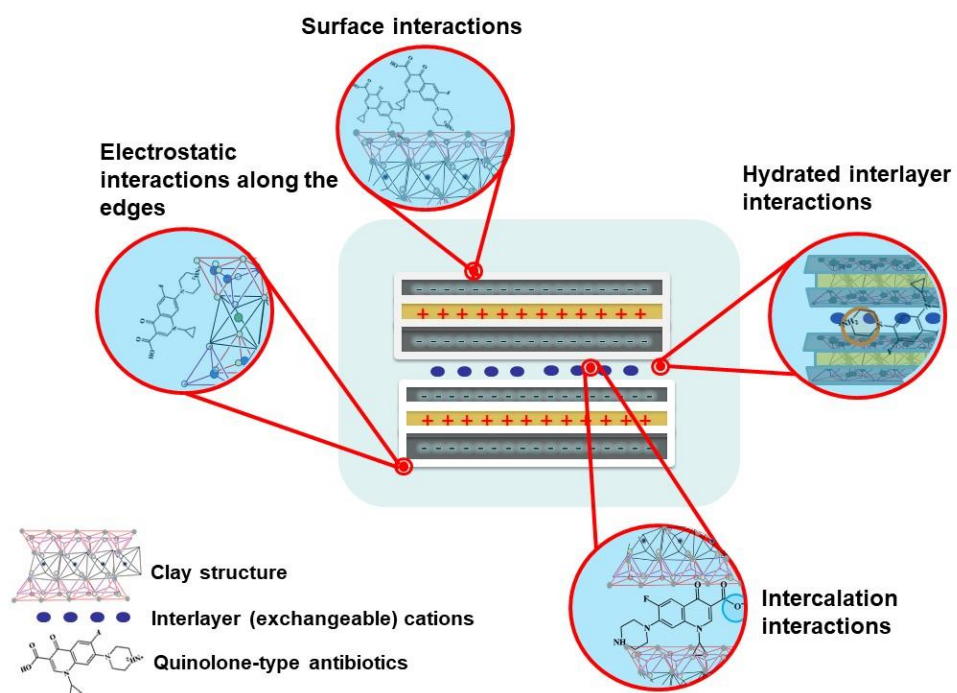


Figure 5: Predominant interactions of FQ-antibiotics with clay minerals

3.2.2. Carbon composites

The limitations of carbon-based sorbents including its intrinsic properties such as large surface area, well-developed porous structures and richness in the surface functional groups led to the synthesis of better adsorbents for the removal of antibiotics from aqueous systems [165,166]. Limitations, as mentioned, also existed for adsorption of ionizable compounds as FQ antibiotics. Similar shortcomings are observed for pristine clay adsorbents for the FQ antibiotics removal. Purely carbon-based adsorbents or only clay were not efficient in the complete removal of FQ. These two sets of adsorbents have their unique properties – when they are combined, FQ is removed with a greater performance by exploiting characteristics of both the materials. In our previous study, we explained the simultaneous interactions of CPX with BC derived from municipal solid waste, where the interactions exist between the oxyanions present at the sorbent sites and the CPX antibiotics at pH 6. The sorption affinity increased with the incorporation of clay to the BC [17,120]. This increase is attributed to the structure of the clay incorporated in the BC lattice that enables additional interactions to take place such as intercalation interactions and electrostatic attractions.

Biochar is capable of high dispersion in aqueous media and has the capacity to stabilize foreign materials within its pores such as clays [120,167] and inorganic metal nanoparticles such as nanoscale zero-valent iron (nZVI) [118,168]. Mao et al. (2019) studied the removal of CPX using BC supported nanoscale zero-valent iron (BC-nZVI) and the results demonstrated high CPX degradation at acidic pH 3-5. Hydrogen peroxide modified BC-nZVI enhanced the degradation further [118,169]. Therefore, multi-functional carbon-based composite has been emphasized to mitigate these limitations [170,171].

Naturally occurring adsorbents like clay minerals have been used in the synthesis of composites with biochar for enhanced removal of FQ from aqueous media [172,173]. Natural attapulgite

with potato stem biochar as a composite was tested for norfloxacin removal and offered a maximum adsorption capacity of 5.24 mg g^{-1} which was almost 2-fold higher than pristine biochar [89] (Table 7). The composite examined [89] exhibited a point of zero charge about 7.55 where the surface was negatively charged at pH higher than the pH_{PZC} and positively charged at pH lower than pH_{PZC} . Since clay minerals have an intrinsic permanent negative charge, their contribution to the composite could be an added advantage for the removal of FQ antibiotics from water [174,175].

Magnetic carbon-based nanocomposites have a marked advantage for their unique properties for the adsorption of FQ-based antibiotics through having a ferric core particle embedded in the interior surrounded by the carbon particles that have a wide range of functional groups [106,176]. In a study on a magnetic carbon-based nanocomposite, sodium chloride was used for investigating the effect of ionic strength on CPX removal. The maximum adsorption capacity was 90.1 mg g^{-1} , and the adsorption was optimum at pH 6-9. Apart from the electrostatic interaction between the protonated and deprotonated CPX at varying pH on the biochar, electron-donor-acceptor interaction played a role in CPX removal. Fluorine in the CPX has a high electron-withdrawing effect with the benzene ring, thereby attractive to the carboxyl anion group on the adsorbent forming the π - π interactions [151,176]. CPX removal efficiency of 87% was achieved with a graphene-oxide-manganese metal-organic framework (MOF) based composite at environmental pH (~5-8) through electrostatic and hydrogen bonding, due to the lower solubility of CPX at this pH range. An optimum adsorption capacity of $1,827 \text{ mg g}^{-1}$ was achieved whereas the PC was as high as 17.63 L g^{-1} [177].

High CPX adsorption capacities were reported for a magnetic nonporous carbon composite with cobalt; the PC was 70 L g^{-1} , illustrating the best performance. Our previous work involved the adsorption of CPX using a composite consisting of biochar, derived from municipal solid

waste and bentonite [178]. The bentonite-biochar mixture was synthesized at a mass ratio of 1:5 and pyrolyzed at 450 °C. An optimal adsorption capacity obtained from this composite was 287 mg g⁻¹ which was around 70% more than the pristine biochar [17,179]. Among the different composites used for the removal of FQ antibiotics, magnetic nanoporous carbon (MNPC) showed the best performance based on the calculated PC value. Both MNPC and graphene illustrated higher performance in removing CPX with chemisorption as the main mechanism. Further studies are needed as published studies on applications of carbon-based composites for the removal of antibiotics are quite rare.

3.2.3. Other nano-based composites

Nano-based composites have been assessed for their removal ability of FQ antibiotics. Among them are clay-based, iron nano-particle, and nano-titanium oxide chitosan composites. The primary aim for the preparation of nano-based composites is to enhance the dispersibility of the parent nanomaterial and improve the specific surface area of the adsorbents with increased functionalities. Thus, enhancing a selective route for the adsorption to take place for FQ antibiotics [125,173,180].

The use of metal-organic frameworks (MOFs) has increasingly become prominent in wastewater treatment at laboratory scale studies because of the outstanding properties such as fine porosity, tunability, and large surface to volume ratio [181]. Recently, Chaturvedi et al. (2020) studied the removal of LVX from aqueous streams using iron-based MOFs (MIL-1009Fe). This adsorbent was prepared using a hydrothermal method. The adsorption of LVX obeyed the Freundlich isotherm model and pseudo-second-order kinetic models resulting in multilayer adsorption of LVX and a maximum adsorption capacity of 87 mg g⁻¹. The equilibrium was reached after 8 h at a basic pH with pHPZC at 3.2 [182].

658 Contrary to other intrinsic properties like pH_{PZC} and pH of the solution, adsorption edge data
659 indicated the removal potential of oxytetracycline antibiotic, a tetracycline-type with
660 carboxylic and amide groups similar to that of the FQ molecule and with similar speciation in
661 aqueous media, withhold the same range where the pH_{PZC} lies in the range of 4-7 for the other
662 nano-based composites including MOFs and nano-zerovalent iron. The dominating mechanism
663 involved inner-sphere surface reactions with the existing amide groups present in
664 oxytetracycline [183]. Nano- Fe_3O_4 also binds with the phenolic portion of the antibiotic, along
665 with both the amide groups in the oxytetracycline antibiotics. The same study tested the
666 removal of CPX from aqueous media and the results obtained were unique compared to
667 oxytetracycline. Apart from the inner-sphere coordination interactions with the carboxylic
668 group of the CPX, a bidentate bridging interaction was reported through the infrared spectrum
669 [184,185]. Due to the magnetic effect on the ketonic group of CPX, it is speculated that the
670 mechanism of adsorption is through electrostatic interactions and inner-sphere complexation
671 [183].

672 Adsorption of CPX from aqueous system in the presence of nano-sized Cu^{2+} by magnetic
673 graphene oxide was studied by Li et al. (2019) [134]. The dispersion of Cu^{2+} nanoparticles and
674 graphene oxide in aqueous media enhanced the adsorption by 10-fold [134]. Iron-based
675 nanoparticles are also used for adsorption and can be produced biologically using a plant-based
676 material. Biosynthesized iron nanoparticles were produced by adding the extract of *Euphorbia*
677 *cochinchensis* leaves, abundantly found in Fujian, China; into $FeSO_4$ solution at 2:1 ratio by
678 volume. Dark particles obtained were further dried and identified as iron-based nanoparticles
679 [186]. Weng et al. (2020) studied the simultaneous decontamination of OFX and EFX using
680 these biosynthesized iron-based nanoparticles and obtained around 92% removal of both
681 contaminants [187].

Table 7: FQ adsorption performances, characteristics, mechanisms of various clay minerals and other tailored adsorbents.

Adsorbents	Quinolone	pH _{PZC}	Optimum pH	Q _{max} (mg g ⁻¹)	PC (L g ⁻¹)	Specific Surface area (m ² g ⁻¹)	Best fitted model	Mechanisms postulated	References
Clay-based Adsorbents									
MMT	CPX	Negatively-charged surface	7	128	5.43	72.2	Pseudo second-order kinetic and Temkin isotherm	Electrostatic interaction	[158]
Sepiolite	EFX	-	7.5	112	-	350	Sigmoidal isotherm	Sub-surface interaction	[164]
				132					
MMT	LVX	Negatively-charged surface	7	57	0.92	-	Langmuir, Freundlich and Dubinin-Radushkevitch isotherm fits	Surface complexation with electrostatic interaction	[162]
MMT	CPX	Negatively-charged surface	7.5	128	0.5	-	-	Electrostatic interaction for surface optimized interactions	[158]
Red mud	CPX	-	-	19	0.06	22	Freundlich isotherm and pseudo-second order kinetics	Electrostatic interaction with multi-layers adsorption	[188]
Kaolinite	CPX	8.3	5.5	26.6 mmol kg ⁻¹	-	-	Pseudo second-order kinetic	Electrostatic interaction with surficial intercalation	[97]
MMT	CPX	Negatively charged	5.7	37	0.24	-	-	Electrostatic interaction at zwitterionic state	[189]
Composites									
Graphene oxide composite with manganese-based MOF (Mn-PBA)	CPX	-	7	1826.64	17.63		Langmuir isotherm	hydrogen bonding, hydrophobic surface interaction, electrostatic	[177]

								interaction, and acid-base interaction	
Graphene oxide with soy protein	CPX		4	500	12.34	119.17	Langmuir and Temkin isotherm models	Hydrogen bonding, π - π electron donor interactions with chemisorption	[190]
Rice straw biochar with molybdenum disulfide (MoS₂)	CPX	3.4	6-8	52.75	4.34	610.4	Freundlich isotherm and pseudo-second order	Chemisorption and π - π electron donor interactions	[125]
Magnetic nonporous carbon (MNPC) with Co	CPX	3.6	5	1644	69.68	170.67	Liquid-film diffusion model pseudo-second order kinetic model fits with Langmuir isotherm	Chemisorption interactions with particle diffusion and liquid-film diffusion	[97]
Biochar derived from potato stem, pyrolyzed at 500 °C with Attapulgit	NFX	7.75	4	5.24	0.446	99.43	Pseudo-second order kinetics	monolayer formation when the solid surface reaches saturation and via electrostatic interaction	[89]
Hydrothermal treated glucose and urea with magnetic iron composite	CPX	7.3	6-9	90.1	9.61	17.74	Langmuir isotherm and pseudo-second order kinetic	Electrostatic interaction and π - π interactions	[176]
Municipal solid waste biochar pyrolyzed at 450 °C for 30 min with Bentonite	CPX	5.7	6	286.6	2.01	7	Elovich kinetic model and Hills isotherm	Hydrogen bonds with π - π electron donor interactions and electrostatic attractions	[17]
Other adsorbents									
Functionalized magnetic fullerene nano-composite (FMFN)	CPX	6.4	6	-	-		Pseudo-first and second-order kinetic with intra-particle diffusion	Chemisorption with film diffusion	[191]

Iron nanoparticles (nano-Fe₃O₄)	CPX	6.5	6	0.04 mmol g ⁻¹	-			Inner sphere complexation involved with the changes in the ions	[183]
Red mud Fe₃O₄ nanoparticles	CPX	8	6	111.11	5.76		Freundlich isotherm with pseudo-second-order kinetics	Electrostatic interactions at heterogenic surfaces	[192]
Nitrilotriacetic acid-functionalized magnetic graphene oxide	CPX	7	8	230.57	2.01		Freundlich isotherm with the pseudo-second-order model	Electrostatic and π - π interactions with a bridging mechanism with hydrogen bonds	[193]
TiO₂ nanotube/reduced graphene oxide hydrogel	CPX	-	7	181.8	3.56	138.2		π - π bond and hydrogen bond	[194]
Iron-based MOFs: MIL-100(Fe)	LVX	3.2	9	87.34	5.58	110.49	Freundlich isotherm and pseudo-second-order	Electrostatic interaction	[195]
Nano-zerovalent iron (NZVI) through reduction with polyethylene glycol and supported on zeolite	NFX	3.47	4	54.67	2.74	37.41	Temkin isotherm	Chemisorption with pollutant competing effects.	[195]
	OFX			28.88	2.56	26.48	pseudo-second-order and Elovich competing kinetics models		
Iron nanoparticles	LVX	-	5.8	6.848	0.591	-	Pseudo-second order model and Langmuir isotherm	Chemisorption, exothermic and spontaneous	[196]
Fe₃O₄@SiO₂									
Nano titanium oxide-chitosan and nano-titanium oxide-bentonite (NBent-NTiO₂-Chit)	LVX	-	4	90.91	-	16.385	Langmuir isotherm and pseudo-second-order	Interfering ions compete and thus mono-layer	[197]

Red mud	CPX	-	-	19	0.06	22	Freundlich isotherm and pseudo-second order kinetics	Electrostatic interaction with multi-layers adsorption	[188]
----------------	-----	---	---	----	------	----	--	--	-------

683

684 MMT: montmorillonite, CPX: Ciprofloxacin, LVX: Levofloxacin, EFX: enrofloxacin, NFX: Norfloxacin, OFX: Ofloxacin

4. Mechanisms of adsorptive removal of FQs

Proposed adsorption mechanisms of FQ antibiotics by adsorbents include electrostatic interactions, van der Waals, hydrogen bonding and π - π EDA interactions [21,93,127]. These interactions are plausible due to the presence of functional groups such as -COOH, -OH, -NH₂ in FQ as well as a variety of functional groups present on the surface of adsorbents.

In the case of carbon-based adsorbents, a strong electron-withdrawing capability is directed towards the electronegative fluorine group of the FQ, by which the electron-rich phenyl group of FQ as π electrons acceptors [98,198]. The available oxyanions on the surface of adsorbents like AC or biochar contribute to the physisorption interaction. Electron donor-acceptor interactions occur in the case of AC. Interaction with the functional groups at varying pH, is seen as a predominant mechanism in the presence of carbonium anions on the AC, as studied by Carabineiro et al. (2012) [100,102]. In a study by Hu et al. (2019), modified biochar with ZnO nanoparticles (loaded at different ratios) and biochar derived from camphor leaves were synthesized at different pyrolysis temperatures and used for CPX removal [115]. It was found that at varying solution pH, the sorption affinity of CPX removal is optimal at the zwitterionic state through electrostatic interactions and through π - π stacking from the electron-deficient-rich interactions between the FQ and biochar [127]. The biochar composite contains aromatic rings that have the ability to donate charges leading to cation- π interactions between CPX and biochar with an optimal adsorption capacity of 450 mg g⁻¹ at pH 5 [115] (Table 4).

Carbon-based structures described in this review show a higher adsorption affinity due to the larger π -plane and quite intricate porous structure, where LVX gets easily accommodated onto the adsorption sites and higher mass transfer takes place [199]. LVX has a higher electron density, and this adds an advantage as a π -electron-acceptor unit due to the presence of the electron-withdrawing effect coming from the fluorine of the LVX. This is further supported by

the x-ray photoelectron spectroscopy and the Fourier transform infrared results suggesting that the adsorption is attributed mainly to micropore filling and π - π electron donor-acceptor interactions [116].

For clay-based adsorption of FQs, the swelling capability of MMT is an added advantage, due to the presence of hydroxyl groups on the surface, and the adsorption was enhanced in the presence of cations in the crystalline structure. The net negative charge is induced through the imperfection in the crystal lattice that leads to the adsorption of FQ. The presence of the interlayers of the clay materials provides an additional void to accommodate FQ within the lattices. For these reasons, clay as an adsorbent has been known for the following interactions: cation exchange, cation bridging, and hydrogen bonding along with electrostatic attraction. These interactions are the main mechanisms for the removal of FQ antibiotics by montmorillonite [200,201].

The solution pH also plays an important role in the sorption of FQ antibiotics as it influences the surface charge of the sorbents and the speciation of FQ. In most cases, the amount of FQ uptake increased with increasing pH up to pH 7-8 and showed a plateau or a declination thereafter (pH 9-11). Through the studies reviewed here, adsorption behavior was dominated by speciation in FQ along with the changes in the surface charge through zeta potential before and after adsorption [140,202]. At $\text{pH} < \text{pH}_{\text{PZC}}$, the surface is positively charged while at $\text{pH} > \text{pH}_{\text{PZC}}$ the surface is negatively charged [203]. As studied by Yang et al. (2012), NFX exists as a cation when $\text{pH} < \text{pH}_{\text{PZC}}$ (4.8); the adsorption is minimal due to the repulsive interactions between the surface and NFX [89,204,205].

For both carbon and clay-based adsorbents, the adsorption is dominated by mostly electrostatic interactions and/or hydrophobic attractions at the environmental pH. The occurrence of anionic and cationic charged species through speciation at the environmental pH facilitates the FQ to be more hydrophobic to the adsorbents which thereafter, have a higher tendency for lower

water solubility and high lipophobicity of FQ at pH 7; thereby, lowering affinity with water [206]. The carboxyl-group and piperazinyl group of FQ antibiotic are the proton-binding sites with dissociation constants (pK_a) around 6.0 and 8.0, respectively, providing a higher affinity for the adsorption of these species onto the adsorbents. Carbon-based adsorbents containing rich aromatic groups provide hydrophobic sites for interaction of FQ molecules facilitating the adsorption process. A detailed scheme for carbon and clay-based adsorbents and their major interactions with FQ antibiotics is depicted in Figure 6.

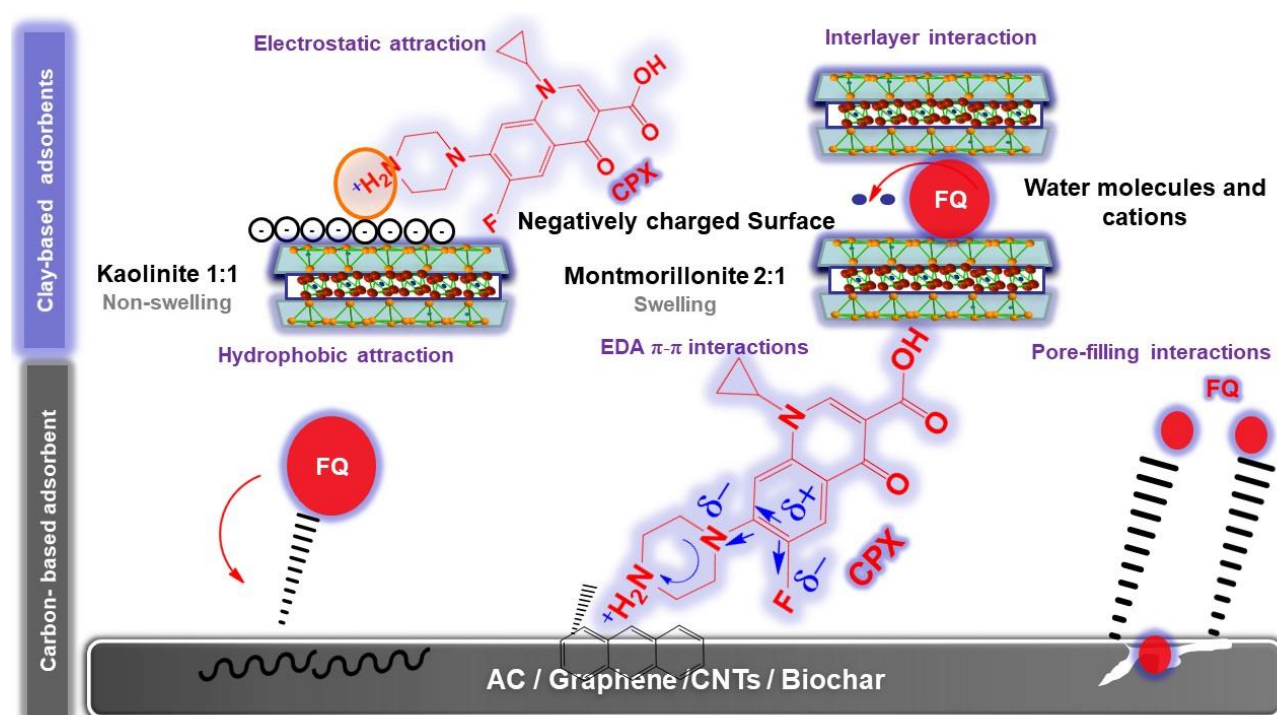


Figure 6: Mechanistic scheme showing the possible interactions between clay-carbon composite adsorbents and FQ antibiotics in aqueous media

5. Performance evaluation of FQ removal

Partition coefficient values are employed in this review to assess the performance of adsorbents more fairly by reducing the bias in adsorption capacity and removal efficiency with the changes in the initial contaminant concentrations [91,207]. Therefore, a comparison of the PC values is

made to understand the true potential of the adsorbents. The PCs of the adsorbents reviewed are illustrated in (Figure 7). Higher PC values indicate enhanced adsorption affinity and ability. The highest PC value was observed for graphene-based adsorbents with an adsorption capacity of 380 mg g^{-1} [130]. A $\text{Fe}_3\text{O}_4/\text{C}$ composite, studied by Mao et al. (2016), showed a lower potential and a lower adsorption capacity than that obtained from graphene with 90.1 mg g^{-1} as adsorption capacity for CPX removal. This removal with a PC value of 9.61 L g^{-1} is attributed to the strong electrostatic interactions between the anionic moiety of CPX and electron-deficient biochar or any other carbon-based adsorbents surface. Moreover, a municipal solid waste biochar-bentonite composite showed an optimum adsorption capacity of 286.6 mg g^{-1} with a lower PC value of 2.01 L g^{-1} compared to the above study [17]. Thus, when considering an adsorbent for decontaminating CPX in aqueous media, as a rule of thumb, the composites outperformed their pristine counterparts and more specifically the $\text{Fe}_3\text{O}_4/\text{C}$ composite exhibits better removal among the composites reviewed here.

Another high performer for the adsorption of FQs is carbon composite with Co [106], which offers a PC value of 69.68 L g^{-1} . This is the highest PC value for the adsorbents reviewed. However, many other factors are required to consider when choosing the adsorbents apart from the manufacturing and the operational cost for actual applications. Table 8 indicates the other aspects of the different adsorbents used for removal of FQ from aqueous systems based on the techno-economical characteristics of each. Commercial activated carbon showed a high CPX adsorption capacity of 131.14 mg g^{-1} but a low PC of 0.661 L g^{-1} [98]. Out of the 7 classes of adsorbents for the removal of FQs antibiotics, the performance based on the PC values is in the following order: graphene > carbon nanotubes > biochar > carbon composite > nano-sorbents > activated carbon > clay-based sorbents.

The performances of different adsorbents are fairly compared based on the PC values for the adsorption of FQ under varying experimental conditions. The difference in the initial

773 conditions utilized in each of the adsorption studies was compensated for comparative
774 purposes, to evaluate the best adsorbents for the removal of FQs. Adsorbents in the studies
775 reviewed here with their PC values could dictate the performance with the FQ antibiotic and
776 should be further evaluated for practical applications including the production costs, economic
777 feasibility, practicability and competitiveness of the adsorbents with the other materials used
778 for the removal of FQ antibiotics from water and wastewater.

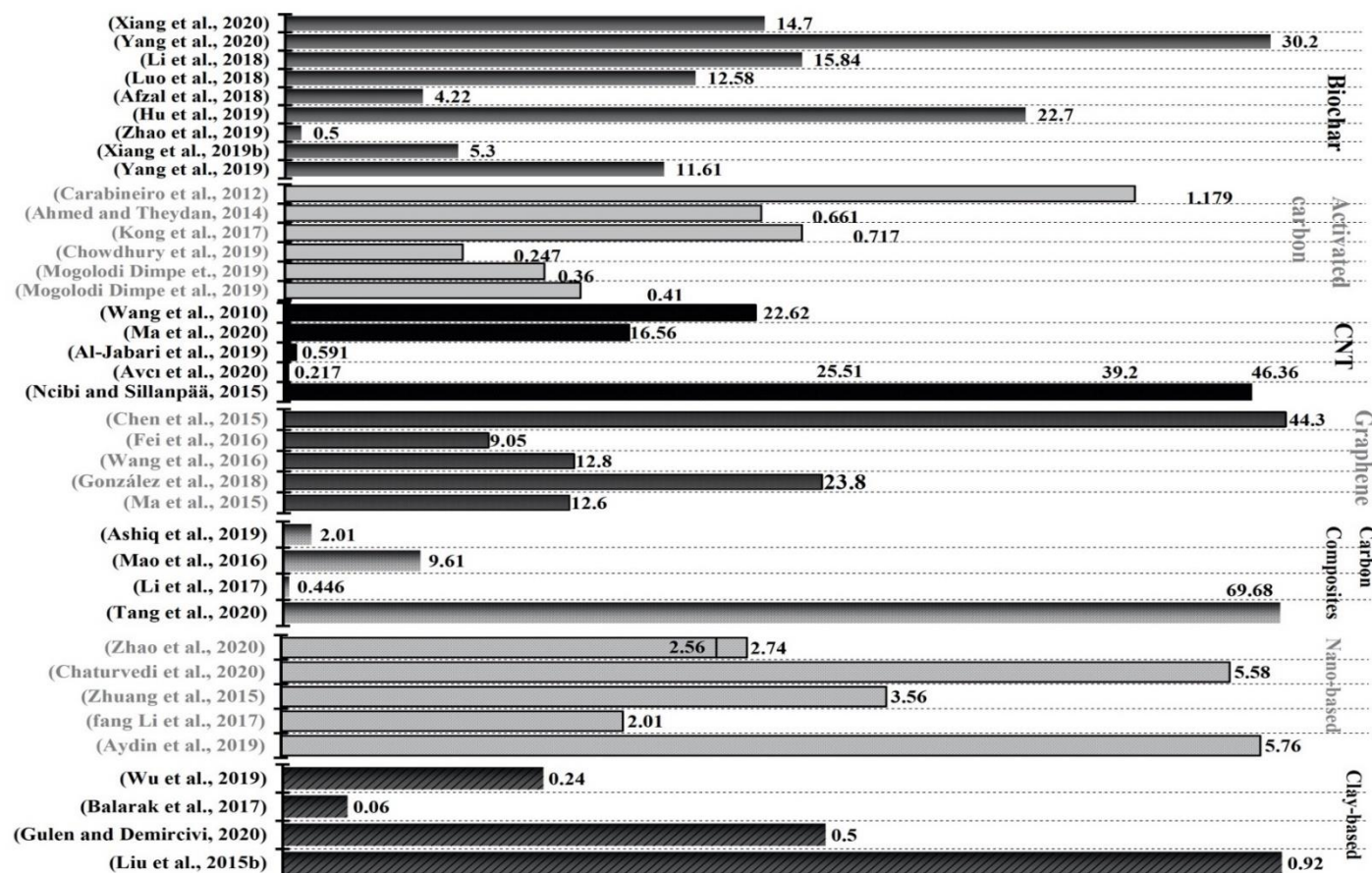


Figure 7: Summary of partition coefficient (L g⁻¹) values for the adsorbent categories reviewed

Note: bars are not to the scale

Table 8: Techno-economic characteristics of different types adsorbents for the remediation of fluoroquinolones in aqueous media

Adsorbents	High pH dependency	High specific area	Multi functionality	Optimal equilibria	Low production cost	Regeneration	Multi-faceted mechanisms	Laboratory scale application	High chemical cost	Handling difficulties
Pristine adsorbents										
Paper sludge Activated carbon	Yes	Yes	No	Yes	No	Yes	No	Yes	No	No
Biochar	Yes	No	Yes	Variable	Yes	No	Yes	No	No	No
Carbon nanotubes	Yes	No	Yes	Variable	No	Yes	Yes	Yes	Yes	Yes
Graphene-oxides	Yes	Yes	No	Variable	No	Variable	Yes	Yes	Yes	Yes
Kaolinite	Yes	No	No	Variable	Yes	No	No	Yes	No	No
Montmorillonite	Yes	Yes	No	Yes	No	No	No	Yes	No	No
Modified/Composites										
Modified Activated carbon	No	Yes	Yes	Yes	No	Yes	Yes	Yes	Yes	Yes
Clay-biochar composite	Yes	No	Yes	Yes	Yes	NS	Yes	Yes	No	No
Magnetic biochar	Variable	Yes	Yes	Yes	Yes	NS	Yes	Yes	Yes	No
Activated biochar	Yes	Yes	Yes	Yes	Yes	Yes	Yes	Yes	Yes	No
Protein modified graphene	No	No	Variable	Variable	No	NS	Yes	Yes	Yes	No
Graphene with magnetic chitosan	No	Yes	Yes	Yes	No	Yes	Yes	Yes	Yes	No

Graphene with sodium alginate	Yes	Yes	Yes	Yes	No	Yes	Yes	Yes	Yes	No
Single-walled carbon nanotubes with graphene	Yes	Yes	Yes	Yes	No	NS	Yes	Yes	Yes	Yes
Multi-walled carbon nanotubes with hydrolyzed treatment	Yes	Yes	Yes	Yes	No	NS	Yes	Yes	Yes	Yes

Note: NS is Not studied for the particular property, variable is varying with different fluoroquinolone studied

6. Conclusions and future perspectives

Adsorbents ranging from biochar to complex materials such as carbon nanotubes are critically analyzed in this review based on their interaction with the FQ antibiotic. Carbon-, nano- and clay-based sorbents are reviewed in great detail and each of them has promising features as well as shortcomings for adsorption of different FQ antibiotics. A very handful of research has been conducted and reported on the performance of these adsorbents through the use of PC as a tool. Therefore, this review detailed out and went further in comparing the performance of adsorbents based on various experimental conditions.

The π - π EDA interactions, electrostatic interactions, and pore-filling are the prominent mechanisms for the adsorption of FQs. However, the mechanisms are dependent on other factors, such as the solution pH, and adsorbent dosage and properties, which also affect the extent of FQ antibiotic adsorption. Carbon-based adsorbents such as activated carbon, graphene, and carbon nanotubes are more homogenous in terms of their structural morphology. Whereas compared to biochar, which is more source-specific, is made of so many different raw materials and thus, the extent of adsorption is dependent on production conditions such as the pyrolysis temperature, yield and activation.

This review categorized the different types of adsorbents and detailed the adsorption process, postulated mechanisms, adsorption studies and adsorbent characteristics for the remediation of FQ antibiotics from aqueous media. Among all various adsorbents discussed here, graphene and CNTs are the best performers and proven to be a proper candidate to adsorb FQ antibiotics from aqueous solutions. Despite being analyzed and reported at a laboratory scale, most of the adsorbents reviewed, except AC, are not applied practically for FQ antibiotic removal at water and wastewater treatment plants due to the lack of reusability studies. Therefore, further investigations over the physical and chemical properties of the materials reviewed here, are

required to fill the gap that leads to field operations for a diversified range of antibiotics including FQ from water and wastewater.

Previous studies did not take into account the complexity of actual environmental scenarios where FQ antibiotics are bounded on different substrates. Several of these interactions are possible apart from electrostatic interactions with carbonaceous adsorbents, clay-based, or composites, making it more challenging to interpret results from different ranges of pH and ions present in the solution. Thus, more studies are needed with systematic experimental approaches that lead to predicting parameters usable for extrapolating the fate of FQs across different pHs and ionic strengths. The surface chemistry of the adsorbents under diversified environmental conditions needs to be elucidated.

Acknowledgments

This work was carried out with the support of Cooperative Research Program for Agriculture Science and Technology Development (Project No. PJ014758), Rural Development Administration, Republic of Korea and the Research Council (ASP/01/RE/SCI/2017/83), Faculty of Applied Sciences, University of Sri Jayewardenepura, Sri Lanka. BS was supported by the Lancaster Environment Centre project.

References

- [1] UN, Sustainable Development Goal 6 Synthesis Report 2018 on Water and Sanitation, United Nations. (2018) 199.
- [2] M. Pan, L.M. Chu, Fate of antibiotics in soil and their uptake by edible crops, *Sci. Total Environ.* 599–600 (2017) 500–512.
<https://doi.org/10.1016/j.scitotenv.2017.04.214>.
- [3] M. Kumar, T. Chaminda, R. Honda, H. Furumai, Vulnerability of urban waters to emerging contaminants in India and Sri Lanka: Resilience framework and strategy,

APN Sci. Bull. 9 (2019). <https://doi.org/10.30852/sb.2019.799>.

[4] P. Grenni, V. Ancona, A. Barra Caracciolo, Ecological effects of antibiotics on natural ecosystems: A review, *Microchem. J.* 136 (2018) 25–39. <https://doi.org/10.1016/j.microc.2017.02.006>.

[5] N. Kemper, Veterinary antibiotics in the aquatic and terrestrial environment, *Ecol. Indic.* 8 (2008) 1–13. <https://doi.org/10.1016/j.ecolind.2007.06.002>.

[6] S.D. Costanzo, J. Murby, J. Bates, Ecosystem response to antibiotics entering the aquatic environment, *Mar. Pollut. Bull.* 51 (2005) 218–223. <https://doi.org/10.1016/j.marpolbul.2004.10.038>.

[7] X. Van Doorslaer, J. Dewulf, H. Van Langenhove, K. Demeestere, Fluoroquinolone antibiotics: An emerging class of environmental micropollutants, *Sci. Total Environ.* 500–501 (2014) 250–269. <https://doi.org/10.1016/j.scitotenv.2014.08.075>.

[8] M. Garcia-Käufer, T. Haddad, M. Bergheim, R. Gminski, P. Gupta, N. Mathur, K. Kümmerer, V. Mersch-Sundermann, Genotoxic effect of ciprofloxacin during photolytic decomposition monitored by the in vitro micronucleus test (MNvit) in HepG2 cells, *Environ. Sci. Pollut. Res.* 19 (2012) 1719–1727. <https://doi.org/10.1007/s11356-011-0686-y>.

[9] J. Kurasam, P. Sihag, P.K. Mandal, S. Sarkar, Presence of fluoroquinolone resistance with persistent occurrence of *gyrA* gene mutations in a municipal wastewater treatment plant in India, *Chemosphere.* 211 (2018) 817–825. <https://doi.org/10.1016/j.chemosphere.2018.08.011>.

[10] G. Sharma, M. Naushad, A.H. Al-Muhtaseb, A. Kumar, M.R. Khan, S. Kalia, Shweta, M. Bala, A. Sharma, Fabrication and characterization of chitosan-crosslinked-poly(alginic acid) nanohydrogel for adsorptive removal of Cr(VI) metal ion from aqueous medium, *Int. J. Biol. Macromol.* 95 (2017) 484–493.

859 <https://doi.org/10.1016/j.ijbiomac.2016.11.072>.

860 [11] G. Sharma, A. Kumar, M. Naushad, A. García-Peñas, A.H. Al-Muhtaseb, A.A. Ghfar,
861 V. Sharma, T. Ahamad, F.J. Stadler, Fabrication and characterization of Gum arabic-
862 cl-poly(acrylamide) nanohydrogel for effective adsorption of crystal violet dye,
863 Carbohydr. Polym. 202 (2018) 444–453.
864 <https://doi.org/10.1016/j.carbpol.2018.09.004>.

865 [12] M. Naushad, G. Sharma, Z.A. Allothman, Photodegradation of toxic dye using Gum
866 Arabic-crosslinked-poly(acrylamide)/Ni(OH)₂/FeOOH nanocomposites hydrogel, J.
867 Clean. Prod. 241 (2019) 118263. <https://doi.org/10.1016/j.jclepro.2019.118263>.

868 [13] C.M. El-Maraghy, O.M. El-Borady, O.A. El-Naem, Effective Removal of
869 Levofloxacin from Pharmaceutical Wastewater Using Synthesized Zinc Oxid, Graphen
870 Oxid Nanoparticles Compared with their Combination, Sci. Rep. 10 (2020) 5914.
871 <https://doi.org/10.1038/s41598-020-61742-4>.

872 [14] M. Zarei, F. Beheshti Nahand, A. Khataee, A. Hasanzadeh, Removal of nalidixic acid
873 from aqueous solutions using a cathode containing three-dimensional graphene, J.
874 Water Process Eng. 32 (2019). <https://doi.org/10.1016/j.jwpe.2019.100978>.

875 [15] T. Wang, X. Pan, W. Ben, J. Wang, P. Hou, Z. Qiang, Adsorptive removal of
876 antibiotics from water using magnetic ion exchange resin, J. Environ. Sci. (China). 52
877 (2017) 111–117. <https://doi.org/10.1016/j.jes.2016.03.017>.

878 [16] M.E. Roca Jalil, M. Baschini, K. Sapag, Influence of pH and antibiotic solubility on
879 the removal of ciprofloxacin from aqueous media using montmorillonite, Appl. Clay
880 Sci. 114 (2015) 69–76. <https://doi.org/10.1016/j.clay.2015.05.010>.

881 [17] A. Ashiq, N.M. Adassooriya, B. Sarkar, A.U. Rajapaksha, Y.S. Ok, M. Vithanage,
882 Municipal solid waste biochar-bentonite composite for the removal of antibiotic
883 ciprofloxacin from aqueous media, J. Environ. Manage. 236 (2019) 428–435.

884 <https://doi.org/10.1016/j.jenvman.2019.02.006>.

885 [18] Y. Xiang, X. Yang, Z. Xu, W. Hu, Y. Zhou, Z. Wan, Y. Yang, Y. Wei, J. Yang,
886 D.C.W. Tsang, Fabrication of sustainable manganese ferrite modified biochar from
887 vinasse for enhanced adsorption of fluoroquinolone antibiotics: Effects and
888 mechanisms, *Sci. Total Environ.* 709 (2020) 136079.
889 <https://doi.org/10.1016/j.scitotenv.2019.136079>.

890 [19] D. Veclani, A. Melchior, Adsorption of ciprofloxacin on carbon nanotubes: Insights
891 from molecular dynamics simulations, *J. Mol. Liq.* 298 (2020) 111977.
892 <https://doi.org/10.1016/j.molliq.2019.111977>.

893 [20] A. Bryskier, J.F. Chantot, Classification and Structure-Activity Relationships of
894 Fluoroquinolones, *Drugs.* 49 (1995) 16–28. [https://doi.org/10.2165/00003495-](https://doi.org/10.2165/00003495-199500492-00005)
895 [199500492-00005](https://doi.org/10.2165/00003495-199500492-00005).

896 [21] L. Riaz, T. Mahmood, A. Khalid, A. Rashid, M.B. Ahmed Siddique, A. Kamal, M.S.
897 Coyne, Fluoroquinolones (FQs) in the environment: A review on their abundance,
898 sorption and toxicity in soil, *Chemosphere.* 191 (2018) 704–720.
899 <https://doi.org/10.1016/j.chemosphere.2017.10.092>.

900 [22] P.C. Appelbaum, P.A. Hunter, The fluoroquinolone antibacterials: Past, present and
901 future perspectives, *Int. J. Antimicrob. Agents.* 16 (2000) 5–15.
902 [https://doi.org/10.1016/S0924-8579\(00\)00192-8](https://doi.org/10.1016/S0924-8579(00)00192-8).

903 [23] S. Thiele-Bruhn, Pharmaceutical antibiotic compounds in soils - A review, *J. Plant*
904 *Nutr. Soil Sci.* 166 (2003) 145–167. <https://doi.org/10.1002/jpln.200390023>.

905 [24] C.L. Amorim, I.S. Moreira, A.S. Maia, M.E. Tiritan, P.M.L. Castro, Biodegradation of
906 ofloxacin, norfloxacin, and ciprofloxacin as single and mixed substrates by *Labrys*
907 *portucalensis* F11, *Appl. Microbiol. Biotechnol.* 98 (2014) 3181–3190.
908 <https://doi.org/10.1007/s00253-013-5333-8>.

- 909 [25] M. Li, D. Wei, Y. Du, Acute toxicity evaluation for quinolone antibiotics and their
 910 chlorination disinfection processes, *J. Environ. Sci. (China)*. 26 (2014) 1837–1842.
 911 <https://doi.org/10.1016/j.jes.2014.06.023>.
- 912 [26] P. Sukul, M. Spiteller, Fluoroquinolone antibiotics in the environment, in: *Rev.*
 913 *Environ. Contam. Toxicol.*, Springer, 2007: pp. 131–162. [https://doi.org/10.1007/978-](https://doi.org/10.1007/978-0-387-69163-3_5)
 914 [0-387-69163-3_5](https://doi.org/10.1007/978-0-387-69163-3_5).
- 915 [27] A. Jia, Y. Wan, Y. Xiao, J. Hu, Occurrence and fate of quinolone and fluoroquinolone
 916 antibiotics in a municipal sewage treatment plant, *Water Res.* 46 (2012) 387–394.
 917 <https://doi.org/10.1016/j.watres.2011.10.055>.
- 918 [28] Y. Yang, W. Song, H. Lin, W. Wang, L. Du, W. Xing, Antibiotics and antibiotic
 919 resistance genes in global lakes: A review and meta-analysis, *Environ. Int.* 116 (2018)
 920 60–73. <https://doi.org/10.1016/j.envint.2018.04.011>.
- 921 [29] N. Dorival-García, A. Zafra-Gómez, A. Navalón, J. González, J.L. Vílchez, Removal
 922 of quinolone antibiotics from wastewaters by sorption and biological degradation in
 923 laboratory-scale membrane bioreactors, *Sci. Total Environ.* 442 (2013) 317–328.
 924 <https://doi.org/10.1016/j.scitotenv.2012.10.026>.
- 925 [30] V. Gómez-Toribio, A.B. García-Martín, M.J. Martínez, Á.T. Martínez, F. Guillén,
 926 Induction of extracellular hydroxyl radical production by white-rot fungi through
 927 quinone redox cycling, *Appl. Environ. Microbiol.* 75 (2009) 3944–3953.
 928 <https://doi.org/10.1128/AEM.02137-08>.
- 929 [31] M. Kumar, B. Ram, H. Sewwandi, Sulfikar, R. Honda, T. Chaminda, Treatment
 930 enhances the prevalence of antibiotic-resistant bacteria and antibiotic resistance genes
 931 in the wastewater of Sri Lanka, and India, *Environ. Res.* 183 (2020) 109179.
 932 <https://doi.org/10.1016/j.envres.2020.109179>.
- 933 [32] C. Roose-Amsaleg, A.M. Laverman, Do antibiotics have environmental side-effects?

934 Impact of synthetic antibiotics on biogeochemical processes, *Environ. Sci. Pollut. Res.*
935 23 (2016) 4000–4012. <https://doi.org/10.1007/s11356-015-4943-3>.

936 [33] J. Tolls, Sorption of veterinary pharmaceuticals in soils: A review, *Environ. Sci.*
937 *Technol.* 35 (2001) 3397–3406. <https://doi.org/10.1021/es0003021>.

938 [34] D. Azanu, B. Styryshave, G. Darko, J.J. Weisser, R.C. Abaidoo, Occurrence and risk
939 assessment of antibiotics in water and lettuce in Ghana, *Sci. Total Environ.* 622–623
940 (2018) 293–305. <https://doi.org/10.1016/j.scitotenv.2017.11.287>.

941 [35] R.M.P. Leal, L.R.F. Alleoni, V.L. Tornisiello, J.B. Regitano, Sorption of
942 fluoroquinolones and sulfonamides in 13 Brazilian soils, *Chemosphere.* 92 (2013)
943 979–985. <https://doi.org/10.1016/j.chemosphere.2013.03.018>.

944 [36] C. ZHANG, Y. FENG, Y. wang LIU, H. qing CHANG, Z. jun LI, J. ming XUE,
945 Uptake and translocation of organic pollutants in plants: A review, *J. Integr. Agric.* 16
946 (2017) 1659–1668. [https://doi.org/10.1016/S2095-3119\(16\)61590-3](https://doi.org/10.1016/S2095-3119(16)61590-3).

947 [37] R.P. Tasho, J.Y. Cho, Veterinary antibiotics in animal waste, its distribution in soil and
948 uptake by plants: A review, *Sci. Total Environ.* 563–564 (2016) 366–376.
949 <https://doi.org/10.1016/j.scitotenv.2016.04.140>.

950 [38] D. Vasudevan, G.L. Bruland, B.S. Torrance, V.G. Upchurch, A.A. MacKay, pH-
951 dependent ciprofloxacin sorption to soils: Interaction mechanisms and soil factors
952 influencing sorption, *Geoderma.* 151 (2009) 68–76.
953 <https://doi.org/10.1016/j.geoderma.2009.03.007>.

954 [39] S. Keerthanan, C. Jayasinghe, J.K. Biswas, M. Vithanage, Pharmaceutical and
955 Personal Care Products (PPCPs) in the environment: Plant uptake, translocation,
956 bioaccumulation, and human health risks, *Crit. Rev. Environ. Sci. Technol.* (2020).
957 <https://doi.org/10.1080/10643389.2020.1753634>.

958 [40] M. Pan, L.M. Chu, Adsorption and degradation of five selected antibiotics in

959 agricultural soil, *Sci. Total Environ.* 545–546 (2016) 48–56.

960 <https://doi.org/10.1016/j.scitotenv.2015.12.040>.

961 [41] M. Pan, C.K.C. Wong, L.M. Chu, Distribution of antibiotics in wastewater-irrigated

962 soils and their accumulation in vegetable crops in the Pearl River Delta, Southern

963 China, *J. Agric. Food Chem.* 62 (2014) 11062–11069.

964 <https://doi.org/10.1021/jf503850v>.

965 [42] T.M. Darweesh, M.J. Ahmed, Adsorption of ciprofloxacin and norfloxacin from

966 aqueous solution onto granular activated carbon in fixed bed column, *Ecotoxicol.*

967 *Environ. Saf.* 138 (2017) 139–145. <https://doi.org/10.1016/j.ecoenv.2016.12.032>.

968 [43] M.D. Celiz, J. Tso, D.S. Aga, Pharmaceutical metabolites in the environment:

969 Analytical challenges and ecological risks, *Environ. Toxicol. Chem.* 28 (2009) 2473–

970 2484. <https://doi.org/10.1897/09-173.1>.

971 [44] M. Lizondo, M. Pons, M. Gallardo, J. Estelrich, Physicochemical properties of

972 enrofloxacin, *J. Pharm. Biomed. Anal.* 15 (1997) 1845–1849.

973 [https://doi.org/10.1016/S0731-7085\(96\)02033-X](https://doi.org/10.1016/S0731-7085(96)02033-X).

974 [45] M. Ashfaq, K.N. Khan, S. Rasool, G. Mustafa, M. Saif-Ur-Rehman, M.F. Nazar, Q.

975 Sun, C.P. Yu, Occurrence and ecological risk assessment of fluoroquinolone

976 antibiotics in hospital waste of Lahore, Pakistan, *Environ. Toxicol. Pharmacol.* 42

977 (2016) 16–22. <https://doi.org/10.1016/j.etap.2015.12.015>.

978 [46] N.H. Tran, M. Reinhard, K.Y.H. Gin, Occurrence and fate of emerging contaminants

979 in municipal wastewater treatment plants from different geographical regions-a

980 review, *Water Res.* 133 (2018) 182–207. <https://doi.org/10.1016/j.watres.2017.12.029>.

981 [47] A. Cuprys, R. Pulicharla, S.K. Brar, P. Drogui, M. Verma, R.Y. Surampalli,

982 Fluoroquinolones metal complexation and its environmental impacts, *Coord. Chem.*

983 *Rev.* 376 (2018) 46–61. <https://doi.org/10.1016/j.ccr.2018.05.019>.

- 984 [48] X.S. Miao, F. Bishay, M. Chen, C.D. Metcalfe, Occurrence of antimicrobials in the
 985 final effluents of wastewater treatment plants in Canada, *Environ. Sci. Technol.* 38
 986 (2004) 3533–3541. <https://doi.org/10.1021/es030653q>.
- 987 [49] K. Noguera-Oviedo, D.S. Aga, Lessons learned from more than two decades of
 988 research on emerging contaminants in the environment, *J. Hazard. Mater.* 316 (2016)
 989 242–251. <https://doi.org/10.1016/j.jhazmat.2016.04.058>.
- 990 [50] R. Hendricks, E.J. Pool, The effectiveness of sewage treatment processes to remove
 991 faecal pathogens and antibiotic residues, *J. Environ. Sci. Heal. - Part A*
 992 *Toxic/Hazardous Subst. Environ. Eng.* 47 (2012) 289–297.
 993 <https://doi.org/10.1080/10934529.2012.637432>.
- 994 [51] F.O. Agunbiade, B. Moodley, Occurrence and distribution pattern of acidic
 995 pharmaceuticals in surface water, wastewater, and sediment of the Msunduzi River,
 996 Kwazulu-Natal, South Africa, *Environ. Toxicol. Chem.* 35 (2016) 36–46.
 997 <https://doi.org/10.1002/etc.3144>.
- 998 [52] Y. Gong, J. Li, Y. Zhang, M. Zhang, X. Tian, A. Wang, Partial degradation of
 999 levofloxacin for biodegradability improvement by electro-Fenton process using an
 1000 activated carbon fiber felt cathode, *J. Hazard. Mater.* 304 (2016) 320–328.
 1001 <https://doi.org/10.1016/j.jhazmat.2015.10.064>.
- 1002 [53] S. Castiglioni, R. Bagnati, D. Calamari, R. Fanelli, E. Zuccato, A multiresidue
 1003 analytical method using solid-phase extraction and high-pressure liquid
 1004 chromatography tandem mass spectrometry to measure pharmaceuticals of different
 1005 therapeutic classes in urban wastewaters, *J. Chromatogr. A.* 1092 (2005) 206–215.
 1006 <https://doi.org/10.1016/j.chroma.2005.07.012>.
- 1007 [54] J. Wilkinson, P.S. Hooda, J. Barker, S. Barton, J. Swinden, Occurrence, fate and
 1008 transformation of emerging contaminants in water: An overarching review of the field,

1009 Environ. Pollut. 231 (2017) 954–970. <https://doi.org/10.1016/j.envpol.2017.08.032>.

1010 [55] M.C. Danner, A. Robertson, V. Behrends, J. Reiss, Antibiotic pollution in surface
 1011 fresh waters: Occurrence and effects, *Sci. Total Environ.* 664 (2019) 793–804.
 1012 <https://doi.org/10.1016/j.scitotenv.2019.01.406>.

1013 [56] S. Rodriguez-Mozaz, S. Chamorro, E. Marti, B. Huerta, M. Gros, A. Sànchez-Melsió,
 1014 C.M. Borrego, D. Barceló, J.L. Balcázar, Occurrence of antibiotics and antibiotic
 1015 resistance genes in hospital and urban wastewaters and their impact on the receiving
 1016 river, *Water Res.* 69 (2015) 234–242. <https://doi.org/10.1016/j.watres.2014.11.021>.

1017 [57] L. Jiang, X. Hu, D. Yin, H. Zhang, Z. Yu, Occurrence, distribution and seasonal
 1018 variation of antibiotics in the Huangpu River, Shanghai, China, *Chemosphere.* 82
 1019 (2011) 822–828. <https://doi.org/10.1016/j.chemosphere.2010.11.028>.

1020 [58] A.J. Watkinson, E.J. Murby, D.W. Kolpin, S.D. Costanzo, The occurrence of
 1021 antibiotics in an urban watershed: From wastewater to drinking water, *Sci. Total*
 1022 *Environ.* 407 (2009) 2711–2723. <https://doi.org/10.1016/j.scitotenv.2008.11.059>.

1023 [59] D.G.J. Larsson, Pollution from drug manufacturing: Review and perspectives, *Philos.*
 1024 *Trans. R. Soc. B Biol. Sci.* 369 (2014) 20130571.
 1025 <https://doi.org/10.1098/rstb.2013.0571>.

1026 [60] M.J. Ahmed, Adsorption of quinolone, tetracycline, and penicillin antibiotics from
 1027 aqueous solution using activated carbons: Review, *Environ. Toxicol. Pharmacol.* 50
 1028 (2017) 1–10. <https://doi.org/10.1016/j.etap.2017.01.004>.

1029 [61] R. Wei, F. Ge, M. Chen, R. Wang, Occurrence of Ciprofloxacin, Enrofloxacin, and
 1030 Florfenicol in Animal Wastewater and Water Resources, *J. Environ. Qual.* 41 (2012)
 1031 1481–1486. <https://doi.org/10.2134/jeq2012.0014>.

1032 [62] A.L. Batt, I.B. Bruce, D.S. Aga, Evaluating the vulnerability of surface waters to
 1033 antibiotic contamination from varying wastewater treatment plant discharges, *Environ.*

1034 Pollut. 142 (2006) 295–302. <https://doi.org/10.1016/j.envpol.2005.10.010>.

1035 [63] J.P. Oliver, C.A. Gooch, S. Lansing, J. Schueler, J.J. Hurst, L. Sassoubre, E.M.
 1036 Crossette, D.S. Aga, Invited review: Fate of antibiotic residues, antibiotic-resistant
 1037 bacteria, and antibiotic resistance genes in US dairy manure management systems, J.
 1038 Dairy Sci. 103 (2020) 1051–1071. <https://doi.org/10.3168/jds.2019-16778>.

1039 [64] J.O. Olatunde, A. Chimezie, B. Tolulope, T.T. Aminat, Determination of
 1040 pharmaceutical compounds in surface and underground water by solid phase
 1041 extraction-liquid chromatography, J. Environ. Chem. Ecotoxicol. 6 (2014) 20–26.
 1042 <https://doi.org/10.5897/jece2013.0312>.

1043 [65] M.J. García-Galán, M. Villagrasa, M.S. Díaz-Cruz, D. Barceló, LC-QqLIT MS
 1044 analysis of nine sulfonamides and one of their acetylated metabolites in the Llobregat
 1045 River basin. Quantitative determination and qualitative evaluation by IDA
 1046 experiments, Anal. Bioanal. Chem. 397 (2010) 1325–1334.
 1047 <https://doi.org/10.1007/s00216-010-3630-y>.

1048 [66] Y.C. Lin, W.W.P. Lai, H. hsin Tung, A.Y.C. Lin, Occurrence of pharmaceuticals,
 1049 hormones, and perfluorinated compounds in groundwater in Taiwan, Environ. Monit.
 1050 Assess. 187 (2015) 256. <https://doi.org/10.1007/s10661-015-4497-3>.

1051 [67] M. Patel, R. Kumar, K. Kishor, T. Mlsna, C.U. Pittman, D. Mohan, Pharmaceuticals of
 1052 emerging concern in aquatic systems: Chemistry, occurrence, effects, and removal
 1053 methods, Chem. Rev. 119 (2019) 3510–3673.
 1054 <https://doi.org/10.1021/acs.chemrev.8b00299>.

1055 [68] Q. Yan, Y.X. Zhang, J. Kang, X.M. Gan, P. Xu-Y, J.S. Guo, X. Gao, A Preliminary
 1056 Study on the Occurrence of Pharmaceutically Active Compounds in the River Basins
 1057 and Their Removal in Two Conventional Drinking Water Treatment Plants in
 1058 Chongqing, China, Clean - Soil, Air, Water. 43 (2015) 794–803.

1059 <https://doi.org/10.1002/clen.201400039>.

1060 [69] T. aus der Beek, F.A. Weber, A. Bergmann, S. Hickmann, I. Ebert, A. Hein, A. Küster,
 1061 Pharmaceuticals in the environment-Global occurrences and perspectives, *Environ.*
 1062 *Toxicol. Chem.* 35 (2016) 823–835. <https://doi.org/10.1002/etc.3339>.

1063 [70] N.H. Tran, L. Hoang, L.D. Nghiem, N.M.H. Nguyen, H.H. Ngo, W. Guo, Q.T. Trinh,
 1064 N.H. Mai, H. Chen, D.D. Nguyen, T.T. Ta, K.Y.H. Gin, Occurrence and risk
 1065 assessment of multiple classes of antibiotics in urban canals and lakes in Hanoi,
 1066 Vietnam, *Sci. Total Environ.* 692 (2019) 157–174.
 1067 <https://doi.org/10.1016/j.scitotenv.2019.07.092>.

1068 [71] M. Sun, M. Ye, J. Wu, Y. Feng, J. Wan, D. Tian, F. Shen, K. Liu, F. Hu, H. Li, X.
 1069 Jiang, L. Yang, F.O. Kengara, Positive relationship detected between soil
 1070 bioaccessible organic pollutants and antibiotic resistance genes at dairy farms in
 1071 Nanjing, Eastern China, *Environ. Pollut.* 206 (2015) 421–428.
 1072 <https://doi.org/10.1016/j.envpol.2015.07.022>.

1073 [72] J.P. Oliver, C.A. Gooch, S. Lansing, J. Schueler, J.J. Hurst, L. Sassoubre, E.M.
 1074 Crossette, D.S. Aga, Invited review: Fate of antibiotic residues, antibiotic-resistant
 1075 bacteria, and antibiotic resistance genes in US dairy manure management systems, *J.*
 1076 *Dairy Sci.* 103 (2020) 1051–1071. <https://doi.org/10.3168/jds.2019-16778>.

1077 [73] M. Motoyama, S. Nakagawa, R. Tanoue, Y. Sato, K. Nomiyama, R. Shinohara,
 1078 Residues of pharmaceutical products in recycled organic manure produced from
 1079 sewage sludge and solid waste from livestock and relationship to their fermentation
 1080 level, *Chemosphere.* 84 (2011) 432–438.
 1081 <https://doi.org/10.1016/j.chemosphere.2011.03.048>.

1082 [74] H. Su, J. Sun, S. Fang, Y. Wei, R. Zheng, Y. Jiang, K. Hu, Effects of lactic acid on
 1083 drug-metabolizing enzymes in Chinese mitten crab (*Eriocheir sinensis*) after oral

1084 enrofloxacin, *Comp. Biochem. Physiol. Part - C Toxicol. Pharmacol.* 223 (2019) 9–14.
 1085 <https://doi.org/10.1016/j.cbpc.2019.04.017>.

1086 [75] L. Zhao, Y.H. Dong, H. Wang, Residues of veterinary antibiotics in manures from
 1087 feedlot livestock in eight provinces of China, *Sci. Total Environ.* 408 (2010) 1069–
 1088 1075. <https://doi.org/10.1016/j.scitotenv.2009.11.014>.

1089 [76] X. Hu, Q. Zhou, Y. Luo, Occurrence and source analysis of typical veterinary
 1090 antibiotics in manure, soil, vegetables and groundwater from organic vegetable bases,
 1091 northern China, *Environ. Pollut.* 158 (2010) 2992–2998.
 1092 <https://doi.org/10.1016/j.envpol.2010.05.023>.

1093 [77] R. Wei, F. Ge, S. Huang, M. Chen, R. Wang, Occurrence of veterinary antibiotics in
 1094 animal wastewater and surface water around farms in Jiangsu Province, China,
 1095 *Chemosphere.* 82 (2011) 1408–1414.
 1096 <https://doi.org/10.1016/j.chemosphere.2010.11.067>.

1097 [78] S. Kuppusamy, D. Kakarla, K. Venkateswarlu, M. Megharaj, Y.E. Yoon, Y.B. Lee,
 1098 Veterinary antibiotics (VAs) contamination as a global agro-ecological issue: A
 1099 critical view, *Agric. Ecosyst. Environ.* 257 (2018) 47–59.
 1100 <https://doi.org/10.1016/j.agee.2018.01.026>.

1101 [79] A. Karci, I.A. Balcioglu, Investigation of the tetracycline, sulfonamide, and
 1102 fluoroquinolone antimicrobial compounds in animal manure and agricultural soils in
 1103 Turkey, *Sci. Total Environ.* 407 (2009) 4652–4664.
 1104 <https://doi.org/10.1016/j.scitotenv.2009.04.047>.

1105 [80] B.I. Escher, K. Fenner, Recent advances in environmental risk assessment of
 1106 transformation products, *Environ. Sci. Technol.* 45 (2011) 3835–3847.
 1107 <https://doi.org/10.1021/es1030799>.

1108 [81] J. Wang, S. Wang, Removal of pharmaceuticals and personal care products (PPCPs)

1109 from wastewater: A review, *J. Environ. Manage.* 182 (2016) 620–640.
 1110 <https://doi.org/10.1016/j.jenvman.2016.07.049>.

1111 [82] A. Ezzariai, M. Hafidi, A. Khadra, Q. Aemig, L. El Fels, M. Barret, G. Merlina, D.
 1112 Patureau, E. Pinelli, Human and veterinary antibiotics during composting of sludge or
 1113 manure: Global perspectives on persistence, degradation, and resistance genes, *J.*
 1114 *Hazard. Mater.* 359 (2018) 465–481. <https://doi.org/10.1016/j.jhazmat.2018.07.092>.

1115 [83] B. Li, T. Zhang, Biodegradation and adsorption of antibiotics in the activated sludge
 1116 process, *Environ. Sci. Technol.* 44 (2010) 3468–3473.
 1117 <https://doi.org/10.1021/es903490h>.

1118 [84] B. Li, T. Zhang, Biodegradation and adsorption of antibiotics in the activated sludge
 1119 process, *Environ. Sci. Technol.* 44 (2010) 3468–3473.
 1120 <https://doi.org/10.1021/es903490h>.

1121 [85] N. Dorival-García, A. Zafra-Gómez, A. Navalón, J. González-López, E. Hontoria, J.L.
 1122 Vílchez, Removal and degradation characteristics of quinolone antibiotics in
 1123 laboratory-scale activated sludge reactors under aerobic, nitrifying and anoxic
 1124 conditions, *J. Environ. Manage.* 120 (2013) 75–83.
 1125 <https://doi.org/10.1016/j.jenvman.2013.02.007>.

1126 [86] D.L. Ross, C.M. Riley, Aqueous solubilities of some variously substituted quinolone
 1127 antimicrobials, *Int. J. Pharm.* 63 (1990) 237–250. [https://doi.org/10.1016/0378-](https://doi.org/10.1016/0378-5173(90)90130-V)
 1128 [5173\(90\)90130-V](https://doi.org/10.1016/0378-5173(90)90130-V).

1129 [87] M.J. Martínez-Mejía, I. Sato, S. Rath, Sorption mechanism of enrofloxacin on humic
 1130 acids extracted from Brazilian soils, *Environ. Sci. Pollut. Res.* 24 (2017) 15995–
 1131 16006. <https://doi.org/10.1007/s11356-017-9210-3>.

1132 [88] H. Peng, B. Pan, M. Wu, R. Liu, D. Zhang, D. Wu, B. Xing, Adsorption of ofloxacin
 1133 on carbon nanotubes: Solubility, pH and cosolvent effects, *J. Hazard. Mater.* 211–212

1134 (2012) 342–348. <https://doi.org/10.1016/j.jhazmat.2011.12.063>.

1135 [89] Y. Li, Z. Wang, X. Xie, J. Zhu, R. Li, T. Qin, Removal of Norfloxacin from aqueous
 1136 solution by clay-biochar composite prepared from potato stem and natural attapulgite,
 1137 Colloids Surfaces A Physicochem. Eng. Asp. 514 (2017) 126–136.
 1138 <https://doi.org/10.1016/j.colsurfa.2016.11.064>.

1139 [90] H.C. Hu, X.S. Chai, D. Barnes, Determination of solid-liquid partition coefficient of
 1140 volatile compounds by solid phase ratio variation based headspace analysis, Fluid
 1141 Phase Equilib. 380 (2014) 76–81. <https://doi.org/10.1016/j.fluid.2014.07.040>.

1142 [91] K. Vikrant, K.H. Kim, Nanomaterials for the adsorptive treatment of Hg(II) ions from
 1143 water, Chem. Eng. J. 358 (2019) 264–282. <https://doi.org/10.1016/j.cej.2018.10.022>.

1144 [92] Y. Xiang, Z. Xu, Y. Wei, Y. Zhou, X. Yang, Y. Yang, J. Yang, J. Zhang, L. Luo, Z.
 1145 Zhou, Carbon-based materials as adsorbent for antibiotics removal: Mechanisms and
 1146 influencing factors, J. Environ. Manage. 237 (2019) 128–138.
 1147 <https://doi.org/10.1016/j.jenvman.2019.02.068>.

1148 [93] M.B. Ahmed, J.L. Zhou, H.H. Ngo, W. Guo, M.A.H. Johir, K. Sornalingam, Single
 1149 and competitive sorption properties and mechanism of functionalized biochar for
 1150 removing sulfonamide antibiotics from water, Chem. Eng. J. 311 (2017) 348–358.
 1151 <https://doi.org/10.1016/j.cej.2016.11.106>.

1152 [94] V. Kårelid, G. Larsson, B. Björleinius, Pilot-scale removal of pharmaceuticals in
 1153 municipal wastewater: Comparison of granular and powdered activated carbon
 1154 treatment at three wastewater treatment plants, J. Environ. Manage. 193 (2017) 491–
 1155 502. <https://doi.org/10.1016/j.jenvman.2017.02.042>.

1156 [95] Y. Chen, D. An, S. Sun, J. Gao, L. Qian, Reduction and removal of chromium VI in
 1157 water by powdered activated carbon, Materials (Basel). 11 (2018) 269.
 1158 <https://doi.org/10.3390/ma11020269>.

- 1159 [96] L. Liu, X. Chen, Z. Wang, S. Lin, Removal of aqueous fluoroquinolones with multi-
 1160 functional activated carbon (MFAC) derived from recycled long-root *Eichhornia*
 1161 *crassipes*: batch and column studies, *Environ. Sci. Pollut. Res.* 26 (2019) 34345–
 1162 34356. <https://doi.org/10.1007/s11356-019-06173-z>.
- 1163 [97] M. Bizi, F.E. El Bachra, Evaluation of the ciprofloxacin adsorption capacity of
 1164 common industrial minerals and application to tap water treatment, *Powder Technol.*
 1165 362 (2020) 323–333. <https://doi.org/10.1016/j.powtec.2019.11.047>.
- 1166 [98] M.J. Ahmed, S.K. Theydan, Fluoroquinolones antibiotics adsorption onto microporous
 1167 activated carbon from lignocellulosic biomass by microwave pyrolysis, *J. Taiwan Inst.*
 1168 *Chem. Eng.* 45 (2014) 219–226. <https://doi.org/10.1016/j.jtice.2013.05.014>.
- 1169 [99] H. Fu, X. Li, J. Wang, P. Lin, C. Chen, X. Zhang, I.H. (Mel. Suffet, Activated carbon
 1170 adsorption of quinolone antibiotics in water: Performance, mechanism, and modeling,
 1171 *J. Environ. Sci. (China)*. 56 (2017) 145–152. <https://doi.org/10.1016/j.jes.2016.09.010>.
- 1172 [100] S. Chowdhury, J. Sikder, T. Mandal, G. Halder, Comprehensive analysis on sorptive
 1173 uptake of enrofloxacin by activated carbon derived from industrial paper sludge, *Sci.*
 1174 *Total Environ.* 665 (2019) 438–452. <https://doi.org/10.1016/j.scitotenv.2019.02.081>.
- 1175 [101] Q. Kong, X. He, L. Shu, M. sheng Miao, Ofloxacin adsorption by activated carbon
 1176 derived from luffa sponge: Kinetic, isotherm, and thermodynamic analyses, *Process*
 1177 *Saf. Environ. Prot.* 112 (2017) 254–264. <https://doi.org/10.1016/j.psep.2017.05.011>.
- 1178 [102] S.A.C. Carabineiro, T. Thavorn-Amornsri, M.F.R. Pereira, P. Serp, J.L. Figueiredo,
 1179 Comparison between activated carbon, carbon xerogel and carbon nanotubes for the
 1180 adsorption of the antibiotic ciprofloxacin, *Catal. Today*. 186 (2012) 29–34.
 1181 <https://doi.org/10.1016/j.cattod.2011.08.020>.
- 1182 [103] S.C.R. Marques, J.M. Marcuzzo, M.R. Baldan, A.S. Mestre, A.P. Carvalho,
 1183 Pharmaceuticals removal by activated carbons: Role of morphology on cyclic thermal

1184 regeneration, Chem. Eng. J. 321 (2017) 233–244.

1185 <https://doi.org/10.1016/j.cej.2017.03.101>.

1186 [104] K. Mogolodi Dimpe, P.N. Nomngongo, Application of activated carbon-decorated

1187 polyacrylonitrile nanofibers as an adsorbent in dispersive solid-phase extraction of

1188 fluoroquinolones from wastewater, J. Pharm. Anal. 9 (2019) 117–126.

1189 <https://doi.org/10.1016/j.jpha.2019.01.003>.

1190 [105] J. Liu, Y. Du, W. Sun, Q. Chang, C. Peng, A granular adsorbent-supported Fe/Ni

1191 nanoparticles activating persulfate system for simultaneous adsorption and degradation

1192 of ciprofloxacin, Chinese J. Chem. Eng. 28 (2020) 1077–1084.

1193 <https://doi.org/10.1016/j.cjche.2019.12.019>.

1194 [106] Y. Tang, Q. Chen, W. Li, X. Xie, W. Zhang, X. Zhang, H. Chai, Y. Huang,

1195 Engineering magnetic N-doped porous carbon with super-high ciprofloxacin

1196 adsorption capacity and wide pH adaptability, J. Hazard. Mater. 388 (2020).

1197 <https://doi.org/10.1016/j.jhazmat.2020.122059>.

1198 [107] B. Wang, Y. song Jiang, F. yun Li, D. yue Yang, Preparation of biochar by

1199 simultaneous carbonization, magnetization and activation for norfloxacin removal in

1200 water, Bioresour. Technol. 233 (2017) 159–165.

1201 <https://doi.org/10.1016/j.biortech.2017.02.103>.

1202 [108] T.M. Darweesh, M.J. Ahmed, Batch and fixed bed adsorption of levofloxacin on

1203 granular activated carbon from date (Phoenix dactylifera L.) stones by KOH chemical

1204 activation, Environ. Toxicol. Pharmacol. 50 (2017) 159–166.

1205 <https://doi.org/10.1016/j.etap.2017.02.005>.

1206 [109] X. Li, S. Chen, X. Fan, X. Quan, F. Tan, Y. Zhang, J. Gao, Adsorption of

1207 ciprofloxacin, bisphenol and 2-chlorophenol on electrospun carbon nanofibers: In

1208 comparison with powder activated carbon, J. Colloid Interface Sci. 447 (2015) 120–

1209 127. <https://doi.org/10.1016/j.jcis.2015.01.042>.

1210 [110] N. Genç, E.C. Dogan, Adsorption kinetics of the antibiotic ciprofloxacin on bentonite,
 1211 activated carbon, zeolite, and pumice, *Desalin. Water Treat.* 53 (2015) 785–793.
 1212 <https://doi.org/10.1080/19443994.2013.842504>.

1213 [111] P. Laganà, G. Caruso, I. Corsi, E. Bergami, V. Venuti, D. Majolino, R. La Ferla, M.
 1214 Azzaro, S. Cappello, Do plastics serve as a possible vector for the spread of antibiotic
 1215 resistance? First insights from bacteria associated to a polystyrene piece from King
 1216 George Island (Antarctica), *Int. J. Hyg. Environ. Health.* 222 (2019) 89–100.
 1217 <https://doi.org/10.1016/j.ijheh.2018.08.009>.

1218 [112] I. Anastopoulos, A. Mittal, M. Usman, J. Mittal, G. Yu, A. Núñez-Delgado, M.
 1219 Kornaros, A review on halloysite-based adsorbents to remove pollutants in water and
 1220 wastewater, *J. Mol. Liq.* 269 (2018) 855–868.
 1221 <https://doi.org/10.1016/j.molliq.2018.08.104>.

1222 [113] W. Liu, J. Zhang, C. Zhang, L. Ren, Sorption of norfloxacin by lotus stalk-based
 1223 activated carbon and iron-doped activated alumina: Mechanisms, isotherms and
 1224 kinetics, *Chem. Eng. J.* 171 (2011) 431–438. <https://doi.org/10.1016/j.cej.2011.03.099>.

1225 [114] X. Yang, X. Zhang, Z. Wang, S. Li, J. Zhao, G. Liang, X. Xie, Mechanistic insights
 1226 into removal of norfloxacin from water using different natural iron ore – biochar
 1227 composites: more rich free radicals derived from natural pyrite-biochar composites
 1228 than hematite-biochar composites, *Appl. Catal. B Environ.* 255 (2019).
 1229 <https://doi.org/10.1016/j.apcatb.2019.117752>.

1230 [115] Y. Hu, Y. Zhu, Y. Zhang, T. Lin, G. Zeng, S. Zhang, Y. Wang, W. He, M. Zhang, H.
 1231 Long, An efficient adsorbent: Simultaneous activated and magnetic ZnO doped
 1232 biochar derived from camphor leaves for ciprofloxacin adsorption, *Bioresour. Technol.*
 1233 288 (2019). <https://doi.org/10.1016/j.biortech.2019.121511>.

- 1234 [116] D. Yang, J. Li, L. Luo, R. Deng, Q. He, Y. Chen, Exceptional levofloxacin removal
1235 using biochar-derived porous carbon sheets: Mechanisms and density-functional-
1236 theory calculation, *Chem. Eng. J.* 387 (2020) 124103.
1237 <https://doi.org/10.1016/j.cej.2020.124103>.
- 1238 [117] J. Li, G. Yu, L. Pan, C. Li, F. You, S. Xie, Y. Wang, J. Ma, X. Shang, Study of
1239 ciprofloxacin removal by biochar obtained from used tea leaves, *J. Environ. Sci.*
1240 (China). 73 (2018) 20–30. <https://doi.org/10.1016/j.jes.2017.12.024>.
- 1241 [118] Q. Mao, Y. Zhou, Y. Yang, J. Zhang, L. Liang, H. Wang, S. Luo, L. Luo, P.
1242 Jeyakumar, Y.S. Ok, M. Rizwan, Experimental and theoretical aspects of biochar-
1243 supported nanoscale zero-valent iron activating H₂O₂ for ciprofloxacin removal from
1244 aqueous solution, *J. Hazard. Mater.* 380 (2019).
1245 <https://doi.org/10.1016/j.jhazmat.2019.120848>.
- 1246 [119] Y. Yan, S. Sun, Y. Song, X. Yan, W. Guan, X. Liu, W. Shi, Microwave-assisted in situ
1247 synthesis of reduced graphene oxide-BiVO₄ composite photocatalysts and their
1248 enhanced photocatalytic performance for the degradation of ciprofloxacin, *J. Hazard.*
1249 *Mater.* 250–251 (2013) 106–114. <https://doi.org/10.1016/j.jhazmat.2013.01.051>.
- 1250 [120] A. Ashiq, B. Sarkar, N. Adassooriya, J. Walpita, A.U. Rajapaksha, Y.S. Ok, M.
1251 Vithanage, Sorption process of municipal solid waste biochar-montmorillonite
1252 composite for ciprofloxacin removal in aqueous media, *Chemosphere.* 236 (2019)
1253 124384. <https://doi.org/10.1016/j.chemosphere.2019.124384>.
- 1254 [121] Y. Xiang, Z. Xu, Y. Zhou, Y. Wei, X. Long, Y. He, D. Zhi, J. Yang, L. Luo, A
1255 sustainable ferromanganese biochar adsorbent for effective levofloxacin removal from
1256 aqueous medium, *Chemosphere.* 237 (2019).
1257 <https://doi.org/10.1016/j.chemosphere.2019.124464>.
- 1258 [122] X. Peng, F. Hu, T. Zhang, F. Qiu, H. Dai, Amine-functionalized magnetic bamboo-

1259 based activated carbon adsorptive removal of ciprofloxacin and norfloxacin: A batch
 1260 and fixed-bed column study, *Bioresour. Technol.* 249 (2018) 924–934.
 1261 <https://doi.org/10.1016/j.biortech.2017.10.095>.

1262 [123] S. Yi, B. Gao, Y. Sun, J. Wu, X. Shi, B. Wu, X. Hu, Removal of levofloxacin from
 1263 aqueous solution using rice-husk and wood-chip biochars, *Chemosphere.* 150 (2016)
 1264 694–701. <https://doi.org/10.1016/j.chemosphere.2015.12.112>.

1265 [124] P. Huang, C. Ge, D. Feng, H. Yu, J. Luo, J. Li, P.J. Strong, A.K. Sarmah, N.S. Bolan,
 1266 H. Wang, Effects of metal ions and pH on ofloxacin sorption to cassava residue-
 1267 derived biochar, *Sci. Total Environ.* 616–617 (2018) 1384–1391.
 1268 <https://doi.org/10.1016/j.scitotenv.2017.10.177>.

1269 [125] Z. Yang, R. Xing, W. Zhou, L. Zhu, Adsorption characteristics of ciprofloxacin onto
 1270 g-MoS₂ coated biochar nanocomposites, *Front. Environ. Sci. Eng.* 14 (2020) 1–10.
 1271 <https://doi.org/10.1007/s11783-019-1218-0>.

1272 [126] J. Zhao, G. Liang, X. Zhang, X. Cai, R. Li, X. Xie, Z. Wang, Coating magnetic
 1273 biochar with humic acid for high efficient removal of fluoroquinolone antibiotics in
 1274 water, *Sci. Total Environ.* 688 (2019) 1205–1215.
 1275 <https://doi.org/10.1016/j.scitotenv.2019.06.287>.

1276 [127] M.Z. Afzal, X.F. Sun, J. Liu, C. Song, S.G. Wang, A. Javed, Enhancement of
 1277 ciprofloxacin sorption on chitosan/biochar hydrogel beads, *Sci. Total Environ.* 639
 1278 (2018) 560–569. <https://doi.org/10.1016/j.scitotenv.2018.05.129>.

1279 [128] J. Luo, X. Li, C. Ge, K. Müller, H. Yu, P. Huang, J. Li, D.C.W. Tsang, N.S. Bolan, J.
 1280 Rinklebe, H. Wang, Sorption of norfloxacin, sulfamerazine and oxytetracycline by
 1281 KOH-modified biochar under single and ternary systems, *Bioresour. Technol.* 263
 1282 (2018) 385–392. <https://doi.org/10.1016/j.biortech.2018.05.022>.

1283 [129] Y. Zhou, S. Cao, C. Xi, X. Li, L. Zhang, G. Wang, Z. Chen, A novel Fe₃O₄/graphene

oxide/citrus peel-derived bio-char based nanocomposite with enhanced adsorption
affinity and sensitivity of ciprofloxacin and sparfloxacin, *Bioresour. Technol.* 292
(2019). <https://doi.org/10.1016/j.biortech.2019.121951>.

[130] H. Chen, B. Gao, H. Li, Removal of sulfamethoxazole and ciprofloxacin from aqueous
solutions by graphene oxide, *J. Hazard. Mater.* 282 (2015) 201–207.
<https://doi.org/10.1016/j.jhazmat.2014.03.063>.

[131] X. Yu, G.L. Zipp, G.W.R. Davidson, The Effect of Temperature and pH on the
Solubility of Quinolone Compounds: Estimation of Heat of Fusion, *Pharm. Res. An
Off. J. Am. Assoc. Pharm. Sci.* 11 (1994) 522–527.
<https://doi.org/10.1023/A:1018910431216>.

[132] Z. Pei, X.Q. Shan, J. Kong, B. Wen, G. Owens, Coadsorption of ciprofloxacin and
Cu(II) on montmorillonite and kaolinite as affected by solution pH, *Environ. Sci.
Technol.* 44 (2010) 915–920. <https://doi.org/10.1021/es902902c>.

[133] S. Park, K.S. Lee, G. Bozoklu, W. Cai, S.B.T. Nguyen, R.S. Ruoff, Graphene oxide
papers modified by divalent ions - Enhancing mechanical properties via chemical
cross-linking, *ACS Nano.* 2 (2008) 572–578. <https://doi.org/10.1021/nn700349a>.

[134] M. fang Li, Y. guo Liu, G. ming Zeng, N. Liu, S. bo Liu, Graphene and graphene-
based nanocomposites used for antibiotics removal in water treatment: A review,
Chemosphere. 226 (2019) 360–380.
<https://doi.org/10.1016/j.chemosphere.2019.03.117>.

[135] S. Kim, C.M. Park, M. Jang, A. Son, N. Her, M. Yu, S. Snyder, D.H. Kim, Y. Yoon,
Aqueous removal of inorganic and organic contaminants by graphene-based
nanoadsorbents: A review, *Chemosphere.* 212 (2018) 1104–1124.
<https://doi.org/10.1016/j.chemosphere.2018.09.033>.

[136] J.A. González, J.G. Bafico, M.E. Villanueva, S.A. Giorgieri, G.J. Copello, Continuous

1309 flow adsorption of ciprofloxacin by using a nanostructured chitin/graphene oxide
 1310 hybrid material, *Carbohydr. Polym.* 188 (2018) 213–220.
 1311 <https://doi.org/10.1016/j.carbpol.2018.02.021>.

1312 [137] K. Sun, S. Dong, Y. Sun, B. Gao, W. Du, H. Xu, J. Wu, Graphene oxide-facilitated
 1313 transport of levofloxacin and ciprofloxacin in saturated and unsaturated porous media,
 1314 *J. Hazard. Mater.* 348 (2018) 92–99. <https://doi.org/10.1016/j.jhazmat.2018.01.032>.

1315 [138] F. Wang, B. Yang, H. Wang, Q. Song, F. Tan, Y. Cao, Removal of ciprofloxacin from
 1316 aqueous solution by a magnetic chitosan grafted graphene oxide composite, *J. Mol.*
 1317 *Liq.* 222 (2016) 188–194. <https://doi.org/10.1016/j.molliq.2016.07.037>.

1318 [139] Y. Fei, Y. Li, S. Han, J. Ma, Adsorptive removal of ciprofloxacin by sodium
 1319 alginate/graphene oxide composite beads from aqueous solution, *J. Colloid Interface*
 1320 *Sci.* 484 (2016) 196–204. <https://doi.org/10.1016/j.jcis.2016.08.068>.

1321 [140] A. Avci, İ. İnci, N. Baylan, Adsorption of ciprofloxacin hydrochloride on multiwall
 1322 carbon nanotube, *J. Mol. Struct.* 1206 (2020).
 1323 <https://doi.org/10.1016/j.molstruc.2020.127711>.

1324 [141] M.C. Ncibi, M. Sillanpää, Optimized removal of antibiotic drugs from aqueous
 1325 solutions using single, double and multi-walled carbon nanotubes, *J. Hazard. Mater.*
 1326 298 (2015) 102–110. <https://doi.org/10.1016/j.jhazmat.2015.05.025>.

1327 [142] J. Ma, Z. Jiang, J. Cao, F. Yu, Enhanced adsorption for the removal of antibiotics by
 1328 carbon nanotubes/graphene oxide/sodium alginate triple-network nanocomposite
 1329 hydrogels in aqueous solutions, *Chemosphere.* 242 (2020).
 1330 <https://doi.org/10.1016/j.chemosphere.2019.125188>.

1331 [143] H. Peng, B. Pan, M. Wu, Y. Liu, D. Zhang, B. Xing, Adsorption of ofloxacin and
 1332 norfloxacin on carbon nanotubes: Hydrophobicity- and structure-controlled process, *J.*
 1333 *Hazard. Mater.* 233–234 (2012) 89–96. <https://doi.org/10.1016/j.jhazmat.2012.06.058>.

- 1334 [144] H. Li, W. Wu, X. Hao, S. Wang, M. You, X. Han, Q. Zhao, B. Xing, Removal of
 1335 ciprofloxacin from aqueous solutions by ionic surfactant-modified carbon nanotubes,
 1336 Environ. Pollut. 243 (2018) 206–217. <https://doi.org/10.1016/j.envpol.2018.08.059>.
- 1337 [145] Q. Gao, W. Chen, Y. Chen, D. Werner, G. Cornelissen, B. Xing, S. Tao, X. Wang,
 1338 Surfactant removal with multiwalled carbon nanotubes, Water Res. 106 (2016) 531–
 1339 538. <https://doi.org/10.1016/j.watres.2016.10.027>.
- 1340 [146] M.A. Alaei Shahmirzadi, S.S. Hosseini, J. Luo, I. Ortiz, Significance, evolution and
 1341 recent advances in adsorption technology, materials and processes for desalination,
 1342 water softening and salt removal, J. Environ. Manage. 215 (2018) 324–344.
 1343 <https://doi.org/10.1016/j.jenvman.2018.03.040>.
- 1344 [147] T.Y. Tan, Z.T. Zeng, G.M. Zeng, J.L. Gong, R. Xiao, P. Zhang, B. Song, W.W. Tang,
 1345 X.Y. Ren, Electrochemically enhanced simultaneous degradation of sulfamethoxazole,
 1346 ciprofloxacin and amoxicillin from aqueous solution by multi-walled carbon nanotube
 1347 filter, Sep. Purif. Technol. 235 (2020). <https://doi.org/10.1016/j.seppur.2019.116167>.
- 1348 [148] Z. Wang, X. Yu, B. Pan, B. Xing, Norfloxacin sorption and its thermodynamics on
 1349 surface-modified carbon nanotubes, Environ. Sci. Technol. 44 (2010) 978–984.
 1350 <https://doi.org/10.1021/es902775u>.
- 1351 [149] B. Sarkar, S. Mandal, Y.F. Tsang, P. Kumar, K.H. Kim, Y.S. Ok, Designer carbon
 1352 nanotubes for contaminant removal in water and wastewater: A critical review, Sci.
 1353 Total Environ. 612 (2018) 561–581. <https://doi.org/10.1016/j.scitotenv.2017.08.132>.
- 1354 [150] Z. Wang, X. Yu, B. Pan, B. Xing, Norfloxacin sorption and its thermodynamics on
 1355 surface-modified carbon nanotubes, Environ. Sci. Technol. 44 (2010) 978–984.
 1356 <https://doi.org/10.1021/es902775u>.
- 1357 [151] H. Li, D. Zhang, X. Han, B. Xing, Adsorption of antibiotic ciprofloxacin on carbon
 1358 nanotubes: PH dependence and thermodynamics, Chemosphere. 95 (2014) 150–155.

- 1359 <https://doi.org/10.1016/j.chemosphere.2013.08.053>.
- 1360 [152] H.M. Ötöker, I. Akmeahmet-Balcioğlu, Adsorption and degradation of enrofloxacin, a
 1361 veterinary antibiotic on natural zeolite, *J. Hazard. Mater.* 122 (2005) 251–258.
 1362 <https://doi.org/10.1016/j.jhazmat.2005.03.005>.
- 1363 [153] P.H. Chang, Z. Li, W.T. Jiang, B. Sarkar, Clay minerals for pharmaceutical
 1364 wastewater treatment, in: *Modif. Clay Zeolite Nanocomposite Mater. Environ. Pharm.*
 1365 *Appl.*, Elsevier, 2018: pp. 167–196. [https://doi.org/10.1016/B978-0-12-814617-](https://doi.org/10.1016/B978-0-12-814617-0.00011-6)
 1366 [0.00011-6](https://doi.org/10.1016/B978-0-12-814617-0.00011-6).
- 1367 [154] S. Dong, Y. Sun, J. Wu, B. Wu, A.E. Creamer, B. Gao, Graphene oxide as filter media
 1368 to remove levofloxacin and lead from aqueous solution, *Chemosphere*. 150 (2016)
 1369 759–764. <https://doi.org/10.1016/j.chemosphere.2015.11.075>.
- 1370 [155] G. Xiong, B. Bin Wang, L.X. You, B.Y. Ren, Y.K. He, F. Ding, I. Dragutan, V.
 1371 Dragutan, Y.G. Sun, Hypervalent silicon-based, anionic porous organic polymers with
 1372 solid microsphere or hollow nanotube morphologies and exceptional capacity for
 1373 selective adsorption of cationic dyes, *J. Mater. Chem. A*. 7 (2019) 393–404.
 1374 <https://doi.org/10.1039/c8ta07109h>.
- 1375 [156] N. Peng, D. Hu, J. Zeng, Y. Li, L. Liang, C. Chang, Superabsorbent Cellulose-Clay
 1376 Nanocomposite Hydrogels for Highly Efficient Removal of Dye in Water, *ACS*
 1377 *Sustain. Chem. Eng.* 4 (2016) 7217–7224.
 1378 <https://doi.org/10.1021/acssuschemeng.6b02178>.
- 1379 [157] Z. Li, H. Hong, L. Liao, C.J. Ackley, L.A. Schulz, R.A. MacDonald, A.L. Mihelich,
 1380 S.M. Emard, A mechanistic study of ciprofloxacin removal by kaolinite, *Colloids*
 1381 *Surfaces B Biointerfaces*. 88 (2011) 339–344.
 1382 <https://doi.org/10.1016/j.colsurfb.2011.07.011>.
- 1383 [158] B. Gulen, P. Demircivi, Adsorption properties of flouroquinolone type antibiotic

1384 ciprofloxacin into 2:1 dioctahedral clay structure: Box-Behnken experimental design,
 1385 J. Mol. Struct. 1206 (2020). <https://doi.org/10.1016/j.molstruc.2019.127659>.
 1386 [159] M.A. Ahsan, M.T. Islam, C. Hernandez, E. Castro, S.K. Katla, H. Kim, Y. Lin, M.L.
 1387 Curry, J. Gardea-Torresdey, J.C. Noveron, Biomass conversion of saw dust to a
 1388 functionalized carbonaceous materials for the removal of Tetracycline,
 1389 Sulfamethoxazole and Bisphenol A from water, J. Environ. Chem. Eng. 6 (2018)
 1390 4329–4338. <https://doi.org/10.1016/j.jece.2018.06.040>.
 1391 [160] Q. Wu, Z. Li, H. Hong, K. Yin, L. Tie, Adsorption and intercalation of ciprofloxacin
 1392 on montmorillonite, Appl. Clay Sci. 50 (2010) 204–211.
 1393 <https://doi.org/10.1016/j.clay.2010.08.001>.
 1394 [161] C. Gu, K.G. Karthikeyan, Sorption of the antimicrobial ciprofloxacin to aluminum and
 1395 iron hydrous oxides, Environ. Sci. Technol. 39 (2005) 9166–9173.
 1396 <https://doi.org/10.1021/es051109f>.
 1397 [162] Y. Liu, C. Dong, H. Wei, W. Yuan, K. Li, Adsorption of levofloxacin onto an iron-
 1398 pillared montmorillonite (clay mineral): Kinetics, equilibrium and mechanism, Appl.
 1399 Clay Sci. 118 (2015) 301–307. <https://doi.org/10.1016/j.clay.2015.10.010>.
 1400 [163] B. Gulen, P. Demircivi, Adsorption properties of flouroquinolone type antibiotic
 1401 ciprofloxacin into 2:1 dioctahedral clay structure: Box-Behnken experimental design,
 1402 J. Mol. Struct. 1206 (2020) 127659. <https://doi.org/10.1016/j.molstruc.2019.127659>.
 1403 [164] M. Sturini, A. Speltini, F. Maraschi, A. Profumo, S. Tarantino, A.F. Gualtieri, M.
 1404 Zema, Removal of fluoroquinolone contaminants from environmental waters on
 1405 sepiolite and its photo-induced regeneration, Chemosphere. 150 (2016) 686–693.
 1406 <https://doi.org/10.1016/j.chemosphere.2015.12.127>.
 1407 [165] R. Zhang, C. Chen, J. Li, X. Wang, Preparation of montmorillonite@carbon composite
 1408 and its application for U(VI) removal from aqueous solution, Appl. Surf. Sci. 349

1409 (2015) 129–137. <https://doi.org/10.1016/j.apsusc.2015.04.222>.

1410 [166] D. Kurnosov, A. Burakov, I. Burakova, Development of a Bentonite Clay/Carbon
 1411 Nanotubes Composite for Liquid-Phase Adsorption, *Mater. Today Proc.* 11 (2019)
 1412 398–403. <https://doi.org/10.1016/j.matpr.2019.01.003>.

1413 [167] K.S.D. Premarathna, A.U. Rajapaksha, B. Sarkar, E.E. Kwon, A. Bhatnagar, Y.S. Ok,
 1414 M. Vithanage, Biochar-based engineered composites for sorptive decontamination of
 1415 water: A review, *Chem. Eng. J.* 372 (2019) 536–550.
 1416 <https://doi.org/10.1016/j.cej.2019.04.097>.

1417 [168] X. Weng, W. Cai, S. Lin, Z. Chen, Degradation mechanism of amoxicillin using clay
 1418 supported nanoscale zero-valent iron, *Appl. Clay Sci.* 147 (2017) 137–142.
 1419 <https://doi.org/10.1016/j.clay.2017.07.023>.

1420 [169] W. Zhang, H. Gao, J. He, P. Yang, D. Wang, T. Ma, H. Xia, X. Xu, Removal of
 1421 norfloxacin using coupled synthesized nanoscale zero-valent iron (nZVI) with H₂O₂
 1422 system: Optimization of operating conditions and degradation pathway, *Sep. Purif.*
 1423 *Technol.* 172 (2017) 158–167. <https://doi.org/10.1016/j.seppur.2016.08.008>.

1424 [170] D. Kerfahi, B.M. Tripathi, D. Singh, H. Kim, S. Lee, J. Lee, J.M. Adams, Effects of
 1425 functionalized and raw multi-walled carbon nanotubes on soil bacterial community
 1426 composition, *PLoS One.* 10 (2015) e0123042.
 1427 <https://doi.org/10.1371/journal.pone.0123042>.

1428 [171] J. Song, S. Zhang, G. Li, Q. Du, F. Yang, Preparation of montmorillonite modified
 1429 biochar with various temperatures and their mechanism for Zn ion removal, *J. Hazard.*
 1430 *Mater.* 391 (2020) 121692. <https://doi.org/10.1016/j.jhazmat.2019.121692>.

1431 [172] V. Gunarathne, A. Ashiq, S. Ramanayaka, P. Wijekoon, M. Vithanage, Biochar
 1432 from municipal solid waste for resource recovery and pollution remediation, *Environ.*
 1433 *Chem. Lett.* 17 (2019) 1225–1235. <https://doi.org/10.1007/s10311-019-00866-0>.

- 1434 [173] K.S.D. Premarathna, A.U. Rajapaksha, B. Sarkar, E.E. Kwon, A. Bhatnagar, Y.S. Ok,
 1435 M. Vithanage, Biochar-based engineered composites for sorptive decontamination of
 1436 water: A review, *Chem. Eng. J.* 372 (2019) 536–550.
 1437 <https://doi.org/10.1016/j.cej.2019.04.097>.
- 1438 [174] B. Sarkar, R. Rusmin, U.C. Ugochukwu, R. Mukhopadhyay, K.M. Manjaiah, Modified
 1439 clay minerals for environmental applications, in: *Modif. Clay Zeolite Nanocomposite*
 1440 *Mater. Environ. Pharm. Appl.*, Elsevier, 2018: pp. 113–127.
 1441 <https://doi.org/10.1016/B978-0-12-814617-0.00003-7>.
- 1442 [175] A.A. Bazrafshan, S. Hajati, M. Ghaedi, Synthesis of regenerable Zn(OH)₂
 1443 nanoparticle-loaded activated carbon for the ultrasound-assisted removal of malachite
 1444 green: optimization, isotherm and kinetics, *RSC Adv.* 5 (2015) 79119–79128.
 1445 <https://doi.org/10.1039/c5ra11742a>.
- 1446 [176] H. Mao, S. Wang, J.Y. Lin, Z. Wang, J. Ren, Modification of a magnetic carbon
 1447 composite for ciprofloxacin adsorption, *J. Environ. Sci. (China)*. 49 (2016) 179–188.
 1448 <https://doi.org/10.1016/j.jes.2016.05.048>.
- 1449 [177] N.A. Khan, T. Najam, S.S.A. Shah, E. Hussain, H. Ali, S. Hussain, A. Shaheen, K.
 1450 Ahmad, M. Ashfaq, Development of Mn-PBA on GO sheets for adsorptive removal of
 1451 ciprofloxacin from water: Kinetics, isothermal, thermodynamic and mechanistic
 1452 studies, *Mater. Chem. Phys.* 245 (2020) 122737.
 1453 <https://doi.org/10.1016/j.matchemphys.2020.122737>.
- 1454 [178] A. Ashiq, N.M. Adassooriya, B. Sarkar, A.U. Rajapaksha, Y.S. Ok, M. Vithanage,
 1455 Municipal solid waste biochar-bentonite composite for the removal of antibiotic
 1456 ciprofloxacin from aqueous media, *J. Environ. Manage.* 236 (2019) 428–435.
 1457 <https://doi.org/10.1016/j.jenvman.2019.02.006>.
- 1458 [179] M. Vithanage, A.U. Rajapaksha, M.S. Bootharaju, T. Pradeep, Surface complexation

1459 of fluoride at the activated nano-gibbsite water interface, *Colloids Surfaces A*
 1460 *Physicochem. Eng. Asp.* 462 (2014) 124–130.
 1461 <https://doi.org/10.1016/j.colsurfa.2014.09.003>.

1462 [180] A.A. Najafpoor, O. Nemati Sani, H. Alidadi, M. Yazdani, A.A. Navaei Fezabady, M.
 1463 Taghavi, Optimization of ciprofloxacin adsorption from synthetic wastewaters using γ -
 1464 Al_2O_3 nanoparticles: An experimental design based on response surface methodology,
 1465 *Colloids Interface Sci. Commun.* 33 (2019) 100212.
 1466 <https://doi.org/10.1016/j.colcom.2019.100212>.

1467 [181] S. Ramanayaka, M. Vithanage, A. Sarmah, T. An, K.H. Kim, Y.S. Ok, Performance of
 1468 metal-organic frameworks for the adsorptive removal of potentially toxic elements in a
 1469 water system: A critical review, *RSC Adv.* 9 (2019) 34359–34376.
 1470 <https://doi.org/10.1039/c9ra06879a>.

1471 [182] G. Chaturvedi, A. Kaur, A. Umar, M.A. Khan, H. Algarni, S.K. Kansal, Removal of
 1472 fluoroquinolone drug, levofloxacin, from aqueous phase over iron based MOFs, MIL-
 1473 100(Fe), *J. Solid State Chem.* 281 (2020) 121029.
 1474 <https://doi.org/10.1016/j.jssc.2019.121029>.

1475 [183] S. Rakshit, D. Sarkar, E.J. Elzinga, P. Punamiya, R. Datta, Mechanisms of
 1476 ciprofloxacin removal by nano-sized magnetite, *J. Hazard. Mater.* 246–247 (2013)
 1477 221–226. <https://doi.org/10.1016/j.jhazmat.2012.12.032>.

1478 [184] D.S. S. Rakshit, P. Punamiya, R. Datta, Sorption of oxytetracycline on magnetite-
 1479 water interface, in: *Geochim. Cosmochim. Acta*, PERGAMON-ELSEVIER SCIENCE
 1480 LTD THE BOULEVARD, LANGFORD LANE, KIDLINGTON ..., 2010: p. A846.

1481 [185] P. Trivedi, D. Vasudevan, Spectroscopic investigation of ciprofloxacin speciation at
 1482 the goethite-water interface, *Environ. Sci. Technol.* 41 (2007) 3153–3158.
 1483 <https://doi.org/10.1021/es061921y>.

- 1484 [186] M. Guo, X. Weng, T. Wang, Z. Chen, Biosynthesized iron-based nanoparticles used as
 1485 a heterogeneous catalyst for the removal of 2,4-dichlorophenol, *Sep. Purif. Technol.*
 1486 175 (2017) 222–228. <https://doi.org/10.1016/j.seppur.2016.11.042>.
- 1487 [187] X. Weng, G. Owens, Z. Chen, Synergetic adsorption and Fenton-like oxidation for
 1488 simultaneous removal of ofloxacin and enrofloxacin using green synthesized Fe NPs,
 1489 *Chem. Eng. J.* 382 (2020) 122871. <https://doi.org/10.1016/j.cej.2019.122871>.
- 1490 [188] D. Balarak, F.K. Mostafapour, A. Joghataei, Kinetics and mechanism of red mud in
 1491 adsorption of ciprofloxacin in aqueous solution, *Biosci. Biotechnol. Res. Commun.* 10
 1492 (2017) 241–248. <https://doi.org/10.21786/bbrc/10.1/35>.
- 1493 [189] M. Wu, S. Zhao, R. Jing, Y. Shao, X. Liu, F. Lv, X. Hu, Q. Zhang, Z. Meng, A. Liu,
 1494 Competitive adsorption of antibiotic tetracycline and ciprofloxacin on
 1495 montmorillonite, *Appl. Clay Sci.* 180 (2019).
 1496 <https://doi.org/10.1016/j.clay.2019.105175>.
- 1497 [190] Y. Zhuang, F. Yu, J. Ma, J. Chen, Adsorption of ciprofloxacin onto graphene-soy
 1498 protein biocomposites, *New J. Chem.* 39 (2015) 3333–3336.
 1499 <https://doi.org/10.1039/c5nj00019j>.
- 1500 [191] N.A. Elessawy, M. Elnouby, M.H. Gouda, H.A. Hamad, N.A. Taha, M. Gouda, M.S.
 1501 Mohy Eldin, Ciprofloxacin removal using magnetic fullerene nanocomposite obtained
 1502 from sustainable PET bottle wastes: Adsorption process optimization, kinetics,
 1503 isotherm, regeneration and recycling studies, *Chemosphere.* 239 (2020) 124728.
 1504 <https://doi.org/10.1016/j.chemosphere.2019.124728>.
- 1505 [192] S. Aydin, M.E. Aydin, F. Beduk, A. Ulvi, Removal of antibiotics from aqueous
 1506 solution by using magnetic Fe₃O₄/red mud-nanoparticles, *Sci. Total Environ.* 670
 1507 (2019) 539–546. <https://doi.org/10.1016/j.scitotenv.2019.03.205>.
- 1508 [193] M. fang Li, Y. guo Liu, S. bo Liu, D. Shu, G. ming Zeng, X. jiang Hu, X. fei Tan, L.

1509 hua Jiang, Z. li Yan, X. xi Cai, Cu(II)-influenced adsorption of ciprofloxacin from
 1510 aqueous solutions by magnetic graphene oxide/nitrilotriacetic acid nanocomposite:
 1511 Competition and enhancement mechanisms, *Chem. Eng. J.* 319 (2017) 219–228.
 1512 <https://doi.org/10.1016/j.cej.2017.03.016>.
 1513 [194] Y. Zhuang, F. Yu, J. Ma, Enhanced Adsorption and Removal of Ciprofloxacin on
 1514 Regenerable Long TiO₂ Nanotube/Graphene Oxide Hydrogel Adsorbents, *J.*
 1515 *Nanomater.* 2015 (2015). <https://doi.org/10.1155/2015/675862>.
 1516 [195] J. Zhao, X. Yang, G. Liang, Z. Wang, S. Li, Z. Wang, X. Xie, Effective removal of
 1517 two fluoroquinolone antibiotics by PEG-4000 stabilized nanoscale zero-valent iron
 1518 supported onto zeolite (PZ-NZVI), *Sci. Total Environ.* 710 (2020) 136289.
 1519 <https://doi.org/10.1016/j.scitotenv.2019.136289>.
 1520 [196] M.H. Al-Jabari, S. Sulaiman, S. Ali, R. Barakat, A. Mubarak, S.A. Khan, Adsorption
 1521 study of levofloxacin on reusable magnetic nanoparticles: Kinetics and antibacterial
 1522 activity, *J. Mol. Liq.* 291 (2019). <https://doi.org/10.1016/j.molliq.2019.111249>.
 1523 [197] M.E. Mahmoud, A.M. El-Ghanam, R.H.A. Mohamed, S.R. Saad, Enhanced adsorption
 1524 of Levofloxacin and Ceftriaxone antibiotics from water by assembled composite of
 1525 nanotitanium oxide/chitosan/nano-bentonite, *Mater. Sci. Eng. C.* 108 (2020) 110199.
 1526 <https://doi.org/10.1016/j.msec.2019.110199>.
 1527 [198] M.F. Carvalho, A.F. Duque, I.C. Gonçalves, P.M.L. Castro, Adsorption of
 1528 fluorobenzene onto granular activated carbon: Isotherm and bioavailability studies,
 1529 *Bioresour. Technol.* 98 (2007) 3424–3430.
 1530 <https://doi.org/10.1016/j.biortech.2006.11.001>.
 1531 [199] B. Yan, C.H. Niu, J. Wang, Analyses of Levofloxacin Adsorption on Pretreated Barley
 1532 Straw with Respect to Temperature: Kinetics, π - π Electron-Donor-Acceptor
 1533 Interaction and Site Energy Distribution, *Environ. Sci. Technol.* 51 (2017) 8048–8056.

1534 <https://doi.org/10.1021/acs.est.7b00327>.

1535 [200] X. Wang, Y. Du, J. Luo, Biopolymer/montmorillonite nanocomposite: Preparation,
 1536 drug-controlled release property and cytotoxicity, *Nanotechnology*. 19 (2008) 65707.
 1537 <https://doi.org/10.1088/0957-4484/19/6/065707>.

1538 [201] L. Mohanambe, S. Vasudevan, Anionic clays containing anti-inflammatory drug
 1539 molecules: Comparison of molecular dynamics simulation and measurements, *J. Phys.*
 1540 *Chem. B*. 109 (2005) 15651–15658. <https://doi.org/10.1021/jp050480m>.

1541 [202] B. Fernández-Reyes, K. Ortiz-Martínez, J.A. Lasalde-Ramírez, A.J. Lasalde-Ramírez,
 1542 Engineered adsorbents for the removal of contaminants of emerging concern from
 1543 water, in: *Contam. Emerg. Concern Water Wastewater Adv. Treat. Process.*, Elsevier,
 1544 2019: pp. 3–45. <https://doi.org/10.1016/B978-0-12-813561-7.00001-8>.

1545 [203] Y. Gao, Q. Yue, B. Gao, Y. Sun, Optimization preparation of activated carbon from
 1546 *Enteromorpha prolifera* using response surface methodology and its adsorption studies
 1547 of fluoroquinolone antibiotics, *Desalin. Water Treat.* 55 (2015) 624–636.
 1548 <https://doi.org/10.1080/19443994.2014.922442>.

1549 [204] W. Yang, Y. Lu, F. Zheng, X. Xue, N. Li, D. Liu, Adsorption behavior and
 1550 mechanisms of norfloxacin onto porous resins and carbon nanotube, *Chem. Eng. J.*
 1551 179 (2012) 112–118. <https://doi.org/10.1016/j.cej.2011.10.068>.

1552 [205] J. Zhang, M. Lu, J. Wan, Y. Sun, H. Lan, X. Deng, Effects of pH, dissolved humic
 1553 acid and Cu²⁺ on the adsorption of norfloxacin on montmorillonite-biochar composite
 1554 derived from wheat straw, *Biochem. Eng. J.* 130 (2018) 104–112.
 1555 <https://doi.org/10.1016/j.bej.2017.11.018>.

1556 [206] J. Ahmad, S. Naeem, M. Ahmad, A.R.A. Usman, M.I. Al-Wabel, A critical review on
 1557 organic micropollutants contamination in wastewater and removal through carbon
 1558 nanotubes, *J. Environ. Manage.* 246 (2019) 214–228.

1559 <https://doi.org/10.1016/j.jenvman.2019.05.152>.

1560 [207] S. Ramanayaka, M. Vithanage, A. Sarmah, T. An, K.H. Kim, Y.S. Ok, Performance of

1561 metal-organic frameworks for the adsorptive removal of potentially toxic elements in a

1562 water system: A critical review, RSC Adv. 9 (2019) 34359–34376.

1563 <https://doi.org/10.1039/c9ra06879a>.

1564

1565